Functions of ornithine decarboxylase (ODC) in mouse ovaries during development and reproduction

Jenna Lowther

Thesis submitted to the University of Ottawa in partial fulfillment of the requirements for the Master's degree in Biochemistry

Biochemistry Department of Biochemistry, Microbiology and Immunology
Faculty of Medicine
University of Ottawa

Abstract

In 1971 it was discovered by Kobayashi *et al* that ovarian activity of ornithine decarboxylase (ODC), the rate-limiting step of the polyamine pathway, increased just prior to ovulation in rats. Following the discovery in rats, this phenomenon of ovarian ODC activity increase was seen in several other mammal species, such as mice and pigs. However, despite this discovery occurring fifty years ago the purpose and function of this activity increase are still unknown. One factor of *Odc* which complicates studies is that whole-body knockouts have been found to be embryonic lethal, with the embryos not making it past embryonic day 3.5. In 2013 our lab found that older mice experienced a smaller ovarian ODC activity increase when compared to their younger counterparts. This decrease in ODC activity corresponded with the increase in reproductive complications typically seen in older mice, such as an increase in miscarriage, and an increased rate of aneuploidies. Furthermore, supplementing the drinking water of these old mice with putrescine, the product of ODC, was found to partially rescue some of these old-age symptoms, such as the rate of miscarriage. In order to further study the purpose of the ovarian ODC rise during the preovulatory period we have generated mice that have had *Odc* knocked out (*Odc*-KO) specifically in the oocytes, or in the granulosa cells. Double knockout mice which had *Odc* knocked out in both the oocytes and granulosa cells were also generated. With these tissue-specific *Odc*-KO mice, it was hypothesized that a lack of *Odc* in the oocytes or granulosa cells would negatively impact the follicular development and fertility of the mice. From the oocyte-specific *Odc*- KO mice we were able to demonstrate that *Odc* expression in the oocyte is not required for oogenesis. Knocking out *Odc* in the oocytes was found to have no effect on the development of the oocyte or the surrounding follicle and, no impact was seen on the fertility of the oocyte-specific *Odc*-KO mice when compared to wild-type controls. The granulosa cell-

specific *Odc*-KO was found to only be a partial knockout. Due to this, the full effects of knocking out *Odc* in the granulosa cells remain inconclusive. More research is required to find a more reliable method of knocking out genes in the granulosa cells in order to study this further. Additionally, more work on the inhibition of gap junctions to prevent the transmission of polyamines throughout the follicle is required to better understand the effects of *Odc* expression and polyamines on reproduction.

Acknowledgements

Firstly, I would like to thank Dr. Johné Liu for taking a chance on me and giving me the opportunity to pursue a master's degree at the University of Ottawa. I would also like to thank the members of my thesis advisory committee, Dr. Barbara Vanderhyden, and Dr. Jay Baltz for their continuous support and feedback throughout this project.

I would like to thank my fellow lab members Ruizhen Li, Dr. Mahdi Mohaqiq and Florence Parweez for all of their help and input with this project. Additionally, I would like to thank Dr. Allison Tscherner and Taylor McClatchie of Dr. Jay Baltz's lab for sharing their oocyte expertise as well as Dr. Ben Tsang's lab for allowing me to use their equipment.

I would like to extend my thanks to the staff of the Animal Care and Veterinary Services of the The University of Ottawa for their continuous support in taking care of our mice and for always being able to answer any questions that I had.

Finally, I'd like to thank my friends and family for listening to me talk about my mice for two years, and my grandmother who was always interested to hear about my research but was not able to see me finish it.

Table of Contents

List of Abbreviations

AGA: 18α-glycyrrhetinic acid

AMA: Advanced Maternal Age

ART: Assisted Reproductive Technology

AZ: Antizyme

AZI: Antizyme Inhibitor

BSA: Bovine Serum Albumin

CBX: Carbenoxolone

cDNA: complementary Deoxyribose Nucleic Acid

COC: Cumulus Cell Complex

Cyp19: Cytochrome P450 family 19 subfamily

Cyp19-iCre: Cytochrome P450 family 19 subfamily-Cre recombinase

DFMO: difluoromethylornithine

DMSO: dimethyl sulfoxide

DNA: Deoxyribonucleic Acid

FACS: Fluorescence Activated Cell Sorting

FSH: Follicle Stimulating Hormone

GC: Granulosa Cell

GDF9: Growth Differentiation Factor 9

GDF9-iCre: Growth Differentiation Factor 9-Cre Recombinase

GV: Germinal Vesicle

GVBD: Germinal Vesicle Breakdown

hCG: human Chorionic Gonadotropin

H&E: Hematoxylin and Eosin

HEPES: N-2-hydroxyethylpiperazine-N-2-ethane sulfonic acid

IHC: Immunohistochemistry

IVF: *In Vitro* Fertilization

IVM: *In Vitro* Maturation

i.p: intraperitoneal

KO: Knock Out

LH: Luteinizing Hormone

mRNA: messenger Ribonucleic Acid

ODC: Ornithine Decarboxylase

PAO: acetylpolyamine oxidase

PBS: Phosphate Buffered Saline

PCR: polymerase chain reaction

PI: Propidium Iodide

PLP: pyridoxal phosphate

PMSG: Pregnant Mare's Serum Gonadotropin

PSSC: Premature Separation of Sister Chromatids

RT-qPCR: Reverse Transcription quantitative Polymerase Chain Reaction

ROS: Reactive Oxygen Species

RT-PCR: Reverse Transcription Polymerase Chain Reaction

SDS: Sodium Dodecyl Sulfate

SDS-PAGE: Sodium Dodecyl-Sulfate PolyAcrylamide Gel Electrophoresis

SSAT: Spermidine/Spermine N1-acetyltransferase

SMO: Spermine Oxidase

TBST: Tris Buffered Saline with Tween

WT: Wild-Type

Table of Figures

Table of Tables

1. Introduction

1.1. Age-based Infertility

Since 2009 Canada's fertility rate has been falling while the average maternal age has been steadily rising. Between 2012 and 2016 the number of children per woman dropped from 1.62 to 1.54. Additionally, the average maternal age steadily rose from 30.3 to 30.8, with the average age of first birth rising from 28.7 to 29.2 [33]. This trend of delaying childbirth is not specific to Canada and can be seen worldwide, such as in the United States, China, and Italy [26]. However, with this steady rise in maternal age, there is also an increased likelihood of complications. As maternal age continues to trend upward, it gets closer to what is considered advanced maternal age (AMA, >35). AMA is associated with an increase in chromosomal abnormalities, miscarriage, pre-term labour, and stillbirth [13].

While many cultural and socioeconomic factors contribute to this increase in maternal age, one contributor is the growing availability of assisted reproductive technology (ART). The CDC defines ART as any fertility treatment where eggs and embryos are handled outside of the woman's body [6]. With this technology, not only are couples experiencing infertility able to try for a baby, but additionally, women who wish to delay childbirth to their later years are able to freeze their eggs. This allows for them to be used at a later date and allows them to circumvent some of the complications that typically come with AMA. Data collected by the CDC on fertility clinics and their success rates highlights the importance of maternal age regarding fertility (Fig. 1). Their data showed that regardless of age patients who used donor eggs or embryos had a live birth rate of approximately 45%. On the other hand, patients who use their own eggs show a decrease in live births as they age, with those who are 45< showing success rates of around 10% [6].

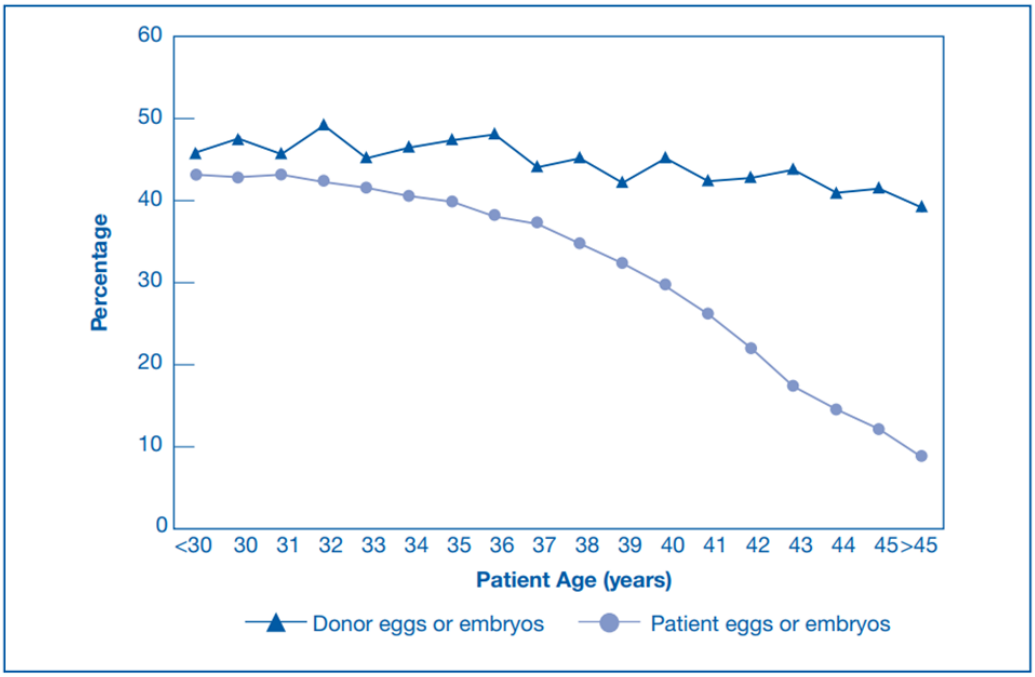

Figure 1. Graph showing the percentage of embryo transfers that resulted in live-birth delivery, by patient age and egg and embryo source in the United States for the year of 2019
Graph showing the percentage of embryo transfers resulting in live births, separated by the use of patient eggs/embryos and donor eggs/embryos. Data shows that no matter the age the use of donor eggs retains its success rate despite the age of the recipient. While the use of patient eggs/embryos results in a decline in success rate as the patient ages.
(Adapted from Centers for Disease Control and Prevention, 2019)

One of the causes of age-based infertility is oocyte depletion via the menstrual cycle. At birth, females are born with a set number of oocytes, and as they age this number decreases. One way oocytes are lost is due to ovulation. When females reach puberty, they begin to undergo the menstrual cycle, within this cycle typically one oocyte will be ovulated every 28 days. However, the majority of oocytes will be lost to programmed cell death, otherwise known as atresia. This programmed cell death continues to occur at a steady pace until the woman reaches the perimenopausal period at around 37 years old, at which point the oocyte reserve begins to deplete more rapidly [24]. The oocyte reserve continues to deplete until the woman reaches menopause, a phenomenon more unique to humans which signals that the oocyte reserve is nearly diminished [16]. The oocytes that are left, in the late reproductive and perimenopausal

period, are characterized for having a higher rate of chromosomal abnormalities. These chromosomal abnormalities can vary from missing chromosomes (monosomy) to having an extra chromosome (trisomy). Chromosomal abnormalities can cause developmental defects and delays in the offspring, such as a trisomy of chromosome 21, otherwise known as Down Syndrome. However, they can also have fatal effects on the embryo, resulting in a miscarriage. This suggests problems occurring during the differentiation of the oocyte, also known as oogenesis [5].

1.2. The Estrus Cycle

While the occurrence of menopause is more unique to humans, the occurrence of age-based infertility is also seen in other species, such as mice, which are frequently used to study reproductive aging. Like humans, oocyte reserves are continuously depleted via ovulation and atresia. However, unlike human females who undergo the menstrual cycle, female mice, as well as many other mammal species, undergo the estrus cycle. This cycle consists of four stages: proestrus, estrus, metestrus, and diestrus. The length of the cycle varies by species, in mice, it lasts four to five days unless interrupted [1]. Mice begin to undergo the estrus cycle after the opening of the vagina which occurs around 26 days after they are born [1].

The estrus cycle begins with the proestrus stage, which corresponds to the follicular phase of the menstrual cycle. This stage lasts 24 hours in mice and is associated with a rise in the circulation of the hormone estradiol, as well as a small surge in the hormone prolactin. This surge in prolactin leads to a rise in luteinizing hormone (LH) and the release of follicle-stimulating hormone (FSH). With the release of FSH, granulosa cell (GC) proliferation is stimulated and select follicles are recruited for ovulation [35]. The larger follicles stimulated into

proliferation by FSH are then able to synthesize aromatase, an enzyme which can convert androgens into estrogen, making estrogen the dominant hormone of this stage [16]. However, not all follicles will receive enough FSH to continue to grow. The follicles that do not receive enough FSH will become atretic and undergo programmed cell death. The rise in LH is very sharp and is referred to as the LH surge. Large dominant follicles gain LH receptors, these receptors allow the oocytes to be released from meiotic prophase arrest [35].

The next stage is the estrus stage which the cycle gets its name from. This stage is the equivalent of the ovulation stage in the menstrual cycle. The estrus stage is when estrogen levels are at their highest and is the only time when the females are receptive to the males for breeding [17]. This stage is also when ovulation takes place. During ovulation, the follicle ruptures allowing the release of the oocyte so that it may travel into the oviduct. In mice, it can take between 12-48 hours to complete. The ruptured follicle that is left behind becomes the corpus luteum. The corpus luteum provides the hormones for the next stage of the estrus cycle, metestrus, which corresponds to the early secretory phase in humans. This cycle is the shortest and ranges from 8-24 hours. Following the release of the oocyte, estrogen levels drop, and progesterone levels rise due to secretions from the corpus luteum. The last stage of the estrus period, diestrus, the equivalent of the late secretory phase, shows the highest levels of progesterone as at this point the corpus luteum has fully formed. Diestrus is the longest of the stages lasting between 48-72 hours in mice. Should fertilization not occur then the corpus luteum regresses, at which point the cycle begins again [1].

1.3. Mammalian Folliculogenesis

As referenced previously, the reproductive system does not only depend on the oocyte but also the follicle [16]. The oocytes are the female germ cells. Each of these oocytes is enclosed within a follicle, with the two being separated by the zona pellucida. The oocyte develops through a process referred to as oogenesis, while the follicle develops through folliculogenesis. Murine follicular development is most often based on the classifications laid out by Pedersen and Peters. Their method looks at the diameter of the oocyte, the layers of GC, as well as the presence of antral fluid to determine the developmental stage. Through their classification follicles can be split up into four major development groups: primordial, primary, secondary, and antral [29].

The follicular development begins with “naked” oocytes that exist in clusters with no GC. At this point in development, they are around 20μm in diameter and are connected to the other oocytes in the cluster via intercellular bridges which allow them to exchange metabolites and organelles [35]. By seven days old most of these clusters of naked oocytes are gone and are replaced by the primordial follicles. These follicles have a single layer of squamous pre-granulosa cells and begin to increase in size [16]. These squamous pre-granulosa cells eventually grow into cuboidal GC which is the benchmark for primary follicles [35].

The primary follicles gain receptors for FSH, which allows them to grow into secondary follicles [16]. Under the influence of FSH, the GC are able to undergo mitosis and differentiate, thus increasing their numbers and the layers of GC. As secondary follicles grow, they begin to form scattered pockets of fluid within the GC. This fluid is referred to as antral fluid, with these follicles also being called preantral follicles. It is during this time that the oocyte reaches its final diameter of approximately 70μm. As the follicle continues to grow these pockets of fluid begin

to coalesce to form the antrum. Once the antrum forms then the follicle is said to have reached the antral stage of development and is referred to as the antral follicle [29]. With the appearance of the antrum, the GC are divided into two types: the cumulus granulosa cells (CC) which surround the oocyte, and the mural granulosa cells, which make up the rest.

The development of the oocyte and the GC that make up the follicle are connected via intercellular membrane channels known as gap junctions. These small channels allow the passage of inorganic ions, second messengers, and metabolites that are less than 1kDa in size. The core unit that makes up these gap junctions are known as connexons, which form hemichannels in the plasma membrane. By placing two connexons of adjacent cells next to each other an intercellular channel forms [19]. Communication between the gap junctions has been shown to be established in fetal ovaries between 19.5 days post coitum to 1 day postpartum [40]. This communication between the granulosa cells and the oocyte ceases when the oocyte is lifted from prophase I arrest [9]. These gap junctions are imperative for the proper development of both the oocyte and the follicle. An example of the gap junctions' effects on the oocyte is their role in maintaining prophase I arrest. The oocyte is kept in meiotic prophase I arrest by high levels of cyclic adenosine monophosphate (cAMP). These high levels of cAMP are maintained by the follicle cells which generate cyclic guanosine monophosphate (cGMP), a second messenger which inhibits phosphodiesterase 3A (PDE3A), an enzyme that breaks down cAMP. cGMP is transferred from the GC into the oocyte via gap junctions in order to inhibit PDE3A and maintain high levels of cAMP. The LH surge is able to release the oocytes from prophase I arrest by reducing cGMP levels, allowing the activation of PDE3A and the breakdown of cAMP [27,43].

The gap junctions also work in the other direction with the oocyte sending signals through for use in follicular development. Growth differentiation factor 9 (GDF9) is a protein specifically synthesized by the oocyte starting in the primordial follicle stage. Research using GDF9-null mice found that while GDF9 is synthesized within the oocyte, its core purpose is for use in GC proliferation. The oocytes of the GDF9-null mice continued to grow to 70μm, however, the GC remained as one layer. In vitro culture also showed that these oocytes lacked meiotic competence with only 40% being able to reach metaphase I or II [8]. This shows how intrinsically related follicular development and oocyte development are. By removing a gene product synthesized in the oocyte you impact follicular development which in turn impacts the oocyte.

1.4. Oogenesis and Meiotic Prophase Arrest

As mentioned previously LH is required to release the oocyte from prophase I arrest. Prophase I is part of the larger process of meiosis. Meiosis is the division of germ cells to reduce chromosome number. Through this process, chromosomes are reduced from 2N to N (diploid to haploid). At the beginning of meiosis, the oocyte consists of two pairs of homologous chromosomes, one inherited from the mother and one inherited from the father. During meiosis, these homologous pairs will come together to exchange genetic information in a process known as homologous recombination. This process ensures that the oocytes will be passing down a new combination of genetic material. When the oocytes transition from the “naked” oocyte clusters and into primordial follicles, they become arrested in the first stage of this process known as prophase I, the stage in which recombination occurs. The arrest occurs at the diplotene substage of prophase I [2]. As previously described, upon being exposed to LH the oocyte is lifted from

prophase I arrest and the germinal vesicle, a membrane which surrounds the nucleus of the oocyte, disintegrates in a process called germinal vesicle breakdown (GVBD). The presence or absence of the germinal vesicle can be observed through a microscope, due to this, oocytes at this stage of development are referred to as GVBD oocytes, while oocytes which still have their germinal vesicle intact are referred to as GV oocytes [16].

Following GVBD, the oocyte can progress through more stages of meiosis: metaphase I, anaphase I, and telophase I. These stages see the now recombined homologous chromosomes organize to the middle of the cell before they are separated to opposite poles of the spindle. Once they have successfully been separated to opposite poles the oocyte begins to asymmetrically divide. This division creates two cells each containing a set of homologous chromosomes. The larger of the cells is the oocyte which will continue to undergo development, the second, much smaller cell, is referred to as the polar body [7]. Through this division, the oocyte is able to extrude one set of homologous chromosomes, while keeping the majority of the organelles and cytoplasm. Like the germinal vesicle, this polar body can also be seen through a microscope and is a benchmark for oocyte development [7].

Following polar body extrusion, the oocyte reassembles a spindle with the remaining set of homologous chromosomes and becomes once again arrested, this time in metaphase II. The oocyte will remain arrested at this stage unless fertilization occurs. Should fertilization occur then the process of meiosis can once again resume, and the oocyte can move onto the last two stages of meiosis, anaphase II and telophase II. During anaphase II the two sister chromatids which make up the homologous chromosome are pulled apart to opposite poles by the spindle. Following this, the cell begins telophase II, which sees the cell asymmetrically divide. Just as in telophase I, one set of sister chromatids remains in the oocyte, while the other is extruded by the

polar body. Following polar body extrusion what remains is a haploid gamete with half of the required genetic material for life. This will then fuse with the pronucleus of the sperm to create one complete set of chromosomes [7].

1.5. Polyamines

Polyamines: putrescine, spermidine and spermine, are three polycationic alkylamines which can be found in all living cells [28]. While spermidine and spermine exist in most cells at millimolar concentrations, putrescine is found in much lower concentrations with some exceptions which will be detailed later [38]. These molecules have been implicated in several essential cell functions, such as cell proliferation, protein synthesis, and RNA/DNA structure, making them essential for cell survival [31]. Due to their wide range of possible functions, polyamines are studied in many disciplines including cancer research, and reproductive research.

1.6. Polyamine Biosynthesis

The synthesis of the polyamines begins with arginine from the urea cycle. Arginine is broken down by arginase to form the amino acid ornithine. From here the enzyme ornithine decarboxylase (ODC) acts on ornithine by removing a carboxyl group to make the first polyamine putrescine, as well as a by-product of CO_2. The conversion of ornithine to putrescine is the rate-limiting step of polyamine biosynthesis. From putrescine, the second polyamine spermidine can be made via enzymatic transfer of an aminopropyl group by spermidine synthase. The final polyamine, spermine, can then be formed through a second enzymatic transfer by spermine synthase (Fig. 2) [23]. This process can also be reversed. Spermidine/spermine N1-acetyltransferase (SSAT) is able to act on spermine to form N^1-Acetylspermine, this is then acted on by acetylpolyamine oxidase (PAO) to form spermidine. This process can then be repeated once again using spermidine to form putrescine [15].

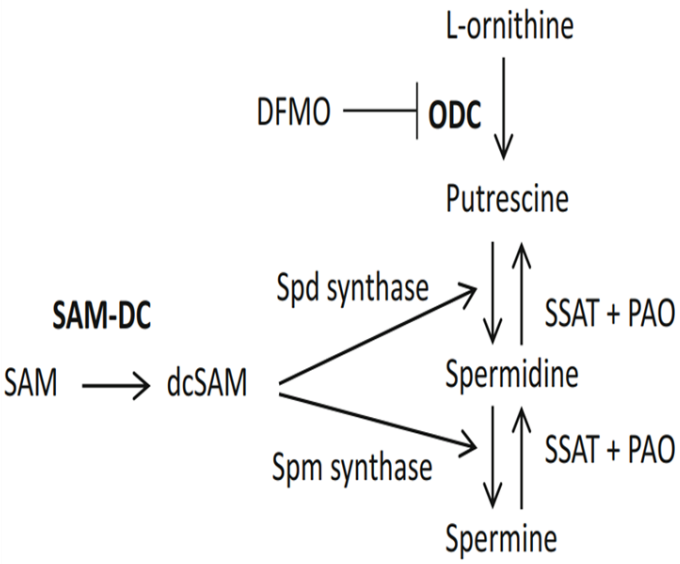

Figure 2. The ODC enzymatic pathway.
The ODC enzymatic pathway starting with the conversion of L-ornithine into putrescine. Sadenosylmethionine decaroxylase (SAM-DC) converts SAM decaroxylated SAM (dcSAM). An amino propyl radical is removed from dcSAM by spermidine (spd) synthase onto putrescine to form spermidine. Spermine synthase then takes an additional amino propyl radical and attaches it to spermidine to form spermine. Within this pathway ODC and SAM-DC are the rate limiting steps. (Adapted from Tao et al., 2019. J Assist Reprod Genet 36:395)

1.7. Ornithine Decarboxylase

As mentioned previously the rate-limiting step of the polyamine pathway is the decarboxylation of ornithine into putrescine, carried out by the enzyme ODC. ODC is a pyridoxal phosphate (PLP) dependent amino acid decarboxylase containing two subunits (homodimer), as well as two active sites [42]. Each subunit contains an NH_2-terminal domain and a COOH terminal domain. The enzyme is then able to form active sites at the boundary of the NH_2-terminal domain of one subunit, and the COOH-terminal domain of the other [30]. A unique attribute of this enzyme is its short half-life, which is thought to be between ten minutes to one hour [42]. The activity of ODC is generally quite low, although activity is known to increase during times of rapid tissue growth, making it a known marker for tumorigenesis, as well during ovulation, and mammalian embryogenesis [11,21,23].

The gene that encodes for this enzyme contains twelve exons and eleven introns. Of these twelve exons, ten contain coding sequences. The ATG start codon resides in exon 3, while the TAG termination sequence is in exon 12. Exons 1 and 2, the first 16 nucleotides of exon 3, as well as what is left of exon 12 following the termination sequence all represent non-coding regions. The protein product is comprised of 461 amino acids [18].

In vivo ODC activity is controlled both by positive and negative feedback mechanisms, with activity being controlled by polyamine concentration [42]. One of the main methods of control is antizyme (AZ), a protein synthesized in response to the ODC activity level [30]. AZ works by binding to ODC, creating the AZ-ODC complex. Non-covalent bonding with AZ then directs ODC to the 26 S proteasome, a protease which degrades protein in the cytosol and nucleus [30,42]. Three forms of AZ have been identified, the first, AZ1, is associated with the degradation of ODC, the second AZ2, is associated with the negative regulation of polyamine

transport, and finally, the third AZ3, which can only be found in the male germ cells [42]. The AZ-ODC complex is reversible as a second protein, antizyme inhibitor (AZI), has a higher affinity for AZ than ODC, releasing ODC from the complex and preventing it from being degraded [42]. ODC can also be controlled via chemical methods. The compound difluoromethylornithine (DFMO), is a substrate-induced irreversible inhibitor of ODC [11]. This works when ODC binds DFMO covalently to form a decarboxylation intermediate but remains trapped [25].

1.8. Functions of Ornithine Decarboxylase in Reproduction

ODC and polyamines have been implicated in reproduction and development in a few different ways. In 1971 it was found that ovarian ODC activity levels rose on the evening of proestrus in rats. Further research of this showed that this activity increase also occurred following the injection of LH, leading researchers to believe that this activity increase was under the control of LH [21]. Inhibition of ODC via DFMO was able to eliminate this rise in activity, as well as the subsequent rise in putrescine. However, only minimal changes to spermine and spermidine were observed. In another experiment, DFMO-treated mice were housed with males for breeding. 10-19 days after the presence of a vaginal plug the females were autopsied, and no effect of the pregnancy was observed between the treated and untreated rats. A decrease was found in the mean viable fetal weight, as well as the placental weight for mice who were treated with DFMO during mating. Additionally, a decrease was seen in the number of implantation sites in mice who were put into mating four days after DFMO treatment [12]. Blocking this rise in ODC on the evening of proestrus using DFMO showed no significant difference in the estrus cycle or the number of ova [4].

Further studies on the effects of ODC activity in ovulation have found that old mice do not experience the same level of ovarian ODC activity rise as their young counterparts [37]. When comparing 8-week-old, 4-month-old, 6-month-old, and 8-month-old mice injected with human chorionic gonadotropin (hCG), the older mice showed lower levels of ODC activity with the 8-month-old mice showing the lowest ODC activity. As previously shown advanced maternal age is associated with reproductive complications such as chromosomal abnormalities. This decrease in ovarian ODC activity corresponds with the AMA phenotype. Additionally, when treating oocytes with DFMO during *in vitro* maturation (IVM), a significant increase was observed in the number of hyperploids in treated oocytes versus control oocytes. The most dominant form of aneuploidy identified was premature separation of sister chromatids (PSSC) [37]. It was also shown that this old age phenotype could be partially rescued via putrescine supplementation [38]. In the oocytes of *Xenopus laevis*, ODC activity transiently rises during oocyte maturation. When ODC translation was blocked in the oocytes using antisense morpholino (xODC mo) oligonucleotides, it was found that it was not required for transition into metaphase II. However, hours after reaching metaphase II the oocytes began to show chromosome disarray, a result of apoptosis. Upon closer inspection it was found that oocytes which had ODC translation disrupted showed higher levels of reactive oxygen species (ROS), suggesting that ODC played a role in its suppression [44].

As stated previously one of the cell functions that ODC has been implicated in is cell proliferation. In addition to this ODC and the subsequent polyamines may play a role in the cell cycle. ODC activity has been found to peak during the G_1/S and G_2/M transition phases of the cell cycle [3]. In cell lines where polyamine synthesis has been inhibited cell proliferation has also been shown to be inhibited. However, this effect has been shown to not be immediate.

Following the administration of inhibitors, it took several cycles for the polyamines to decrease to a level where proliferation could no longer take place. When polyamine levels did reach a point where the cell cycle was stopped, it was found that the cells were arrested at the G_1/S boundary, one of the time points where ODC activity is known to increase [3].

Polyamines being necessary for cell proliferation is also seen in mice that have had the gene for ODC knocked out. *Odc*-null mice were found to not be viable as the embryos could not survive past embryonic day 3.5. At this point the inner cell mass (ICM) of the embryo is no longer able to proliferate, and shortly after the embryo begins to degenerate [32]. Similar results can also be replicated with DFMO. Providing mice 0.5% DFMO in their drinking water between days five and eight of gestation was shown to affect embryogenesis. Mice were autopsied 24 hours prior to their expected due date. Of the mice examined fewer were found to be pregnant in the treated group than in the control group. Of the pregnant mice, there was an average of two viable fetuses compared to 9.8 in the control mice. Accompanying the viable fetuses were reabsorption nodules showing that there were more embryos that did not make it. The treated group also showed a reduction in fetal and placental weight when compared to the control group [11].

1.9. Project objectives and hypothesis

Despite all of this research, the mechanism and overall purpose of the ovarian rise in ODC activity during proestrus are still unknown. In order to further investigate the roles of ODC and polyamines in ovarian development and reproduction, it was decided to breed mice which had *Odc* specifically knocked out (*Odc*-KO) in either the oocytes or the granulosa cells. With these tissue-specific knockouts, we are able to circumvent the embryonic lethality of the whole-body *Odc*-KO and ensure that only the tissues of interest, the oocytes and GC, were affected [32]. This was done using the Cre-LoxP system. Oocyte specificity was achieved using a GDF9 promotor driving Cre expression (*GDF9-iCre*), while GC specificity was achieved using a Cyp19 promotor (*Cyp19-iCre*) With these oocyte-specific *Odc*-KO and GC-specific *Odc*-KO mice, we were looking to see if they expressed a similar or more extreme phenotype to the old age mice [38]. We hypothesized that the lack of ODC activity in the oocytes or GC may affect oocyte growth and/or follicle development. With these *Odc* KO mice, we had two main objectives:

1. To generate oocyte and GC-specific *Odc* knockout mice
2. To determine the reproductive functions of these mice

2. Materials and Methods

2.1. Mice

Animal protocols were approved by the Animal Care Committee of the Ottawa Hospital Research Institute and University of Ottawa (OHRI-3304). Initial *GDF9-iCre* and *Cyp19-iCre* breeders were gifted by the Vanderhyden lab (OHRI), and initial $Odc^{+/Fl}$ breeders were gifted by the Cleveland Lab (Moffitt Cancer Center). Wild-type mice were purchased from Charles River (QC, Canada). Unless specified all the mice used were of C57BL/6 background.

2.2. Cre-loxP Breeding

The KO was achieved using the Cre-loxP system. Two loxP sites were inserted in the *Odc* gene to loop out exon 2 and exon 3 as the ATG start codon resides in exon 3 (Fig. 3) [14]. Tissue specificity was achieved using Cre-recombinase attached to either a GDF9 or a Cyp19 promotor. As mentioned previously GDF9 is a gene specifically expressed in the oocyte for use in the GC and expression starts at a very early stage in oocyte development [8,22]. With *GDF9-iCre* we can knockout *Odc* in the oocytes early in oocyte development. Cyp19 is a gene expressed in the GC and encodes for the enzyme aromatase which is used to convert androgens into estrogen. Due to this, Cyp19 is expressed later in development in the antral follicle stage when the follicles begin to produce estrogen [35]. With *Cyp19-iCre* we are able to knock out *Odc* specifically in the GC, in the antral follicle stage [10].

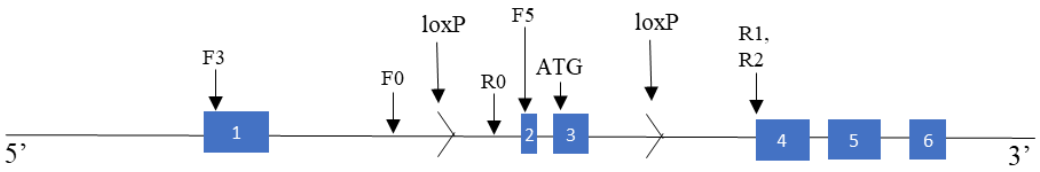

Figure 3. The first six exons of the *Odc*^{Fl} gene with primer locations and ATG start codon indicated.
The first six exons (in blue) of the *Odc*^{Fl} gene with arrows indicating the loxP sites. Locations of PCR and RT-PCR primers also indicated. The ATG start codon in exon 3 is also shown.

To breed the oocyte and GC-specific *Odc*-KO females, males with the genotype *Odc*$^{Fl/Fl}$ who carried the Cre Recombinase transgene (either *GDF9-iCre* or *Cyp19-iCre*) were mated with females with the genotype *Odc*$^{Fl/Fl}$. The offspring from this mating had a 100% chance of inheriting the flox sites and a 50% chance of inheriting the Cre-transgene, with a final probability of 25% in order to breed a female mouse that carried the transgene (Fig. 4). Due to the Cre-transgene only being passed down through the father, resulting knockout mice would only possess one copy of the transgene.

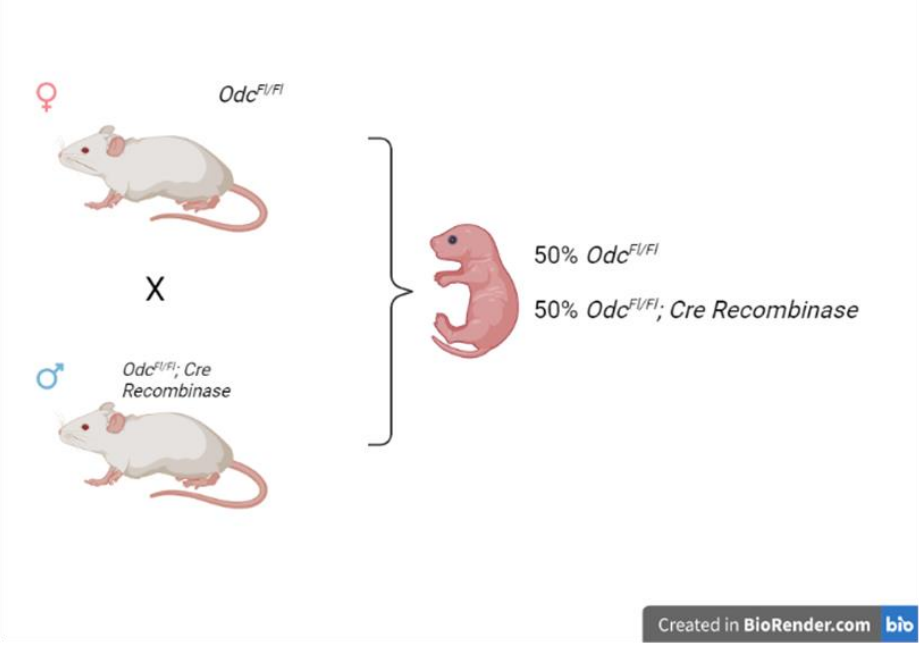

Figure 4. *Odc*$^{Fl/Fl}$; Cre Recombinase mating scheme.
The mating scheme to obtain oocyte and granulosa cell-specific knockouts by breeding an *Odc*$^{Fl/Fl}$ females with *Odc*$^{Fl/Fl}$; *iCre* males. This pairing results in a 50% chance of the pups inheriting the transgene from their father. In order to get a female of the *Odc*$^{Fl/Fl}$; *iCre* genotype the probability is 25%.

In order to breed for GC-Specific *Odc*-KO mice in the background of heterozygous *Odc*, males with the genotype *Odc*$^{Fl/Fl}$; *Cyp19-iCre* were bred with females with the genotype *Odc*$^{+/-}$. With this pairing, the offspring had a 50% chance of being *Odc*$^{Fl/-}$, and a 50% chance of inheriting the transgene from their father. When factoring in gender this pairing had a 12.5% chance of producing females with the genotype *Odc*$^{Fl/-}$; *Cyp19-iCre* (Fig. 4). Oocyte and GC-specific *Odc*-KO mice were generated in a similar fashion, but with the mother carrying *GDF9-iCre* as well. With this pairing, the likelihood of producing a female *Odc*$^{Fl/-}$*; Cyp19-iCre; GDF9-iCre* mouse was 6.25%

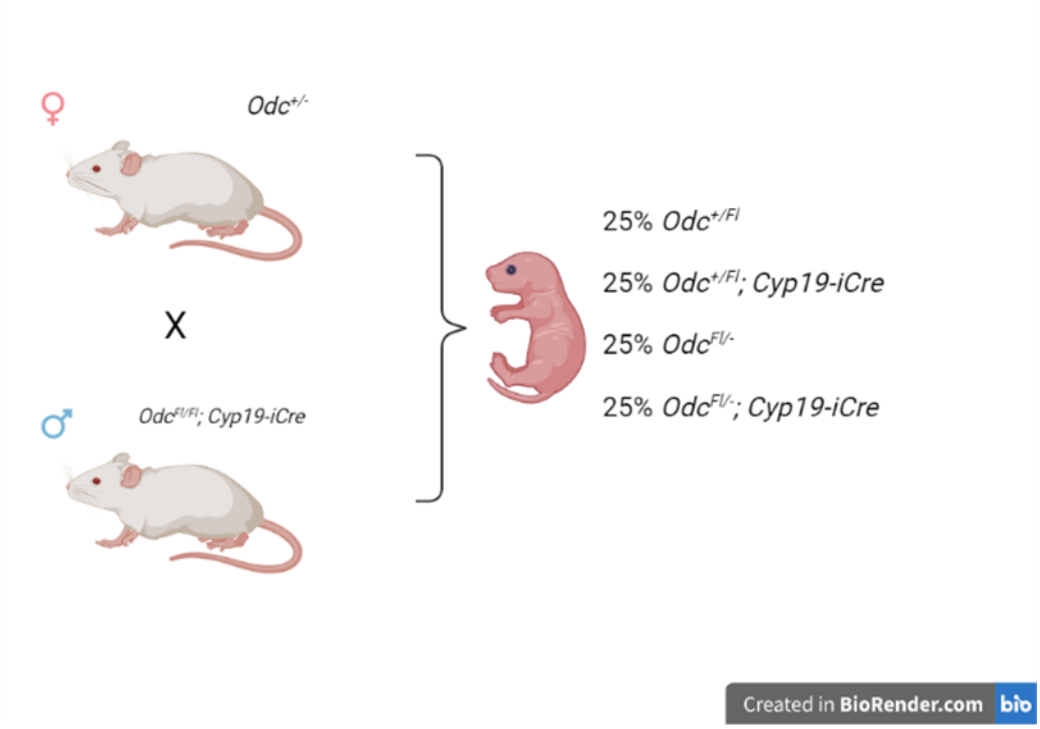

Figure 5. *Odc*$^{Fl/-}$*; Cyp19-iCre* mating scheme.
The mating scheme to obtain granulosa cell-specific knockouts in the background of heterozygous *Odc* by breeding an *Odc*$^{+/-}$ females with *Odc*$^{Fl/Fl}$*; Cyp19-iCre* males. This pairing results in a 25% chance of the pups inheriting both the transgene from their father and the *Odc*$^{-}$ from their mother. In order to get a female of the *Odc*$^{Fl/-}$*; Cyp19-iCre* genotype the probability is 12.5%.

Table 1: Summary of transgenic mice

Name	Genotype
Oocyte-specific Odc-KO	*Odc*$^{Fl/Fl}$*; GDF9-iCre*
Oocyte-specific *Odc*-KO in the background of heterozygous *Odc*	*Odc*$^{Fl/-}$*; GDF9-iCre*
Granulosa cell-specific *Odc*-KO	*Odc*$^{Fl/Fl}$*; Cyp19-iCre*
Granulosa cell specific *Odc*-KO in the background of heterozygous *Odc*	*Odc*$^{Fl/-}$*; Cyp19-iCre*
Oocyte, and GC-Specific Double *Odc*-KO	*Odc*$^{Fl/-}$*; GDF9-iCre; Cyp19-iCre*

2.3. Oocyte Collection

2.3.1. GV/GVBD Collection

To collect GV/GVBD oocytes, females between the ages of four and six weeks were injected intraperitoneally (i.p) with 100µl of 5IU pregnant mare serum gonadotropin (PMSG; ProspecBio, HOR-272) in order to stimulate the maturation of the follicles. 46 hours post-injection the mice were sacrificed via CO_2 inhalation followed by cervical dislocation. The ovaries of the mice were removed and placed into a 3ml dish containing warmed phosphate-buffered saline (PBS; aMResco, E703-1L) and cleaned of fat. Once the fat was removed the ovaries were moved to a new dish of PBS and then punctured using a 30G needle causing the oocytes to be released. Oocytes were collected into a separate drop of PBS using a glass denudation pipette (Vitrolife, 14390). After collection, oocytes were washed three times in PBS to remove any residual granulosa cells before being collected in minimal media and frozen on dry ice. Collected oocytes were stored at -80°C.

2.3.2. Superovulation and the collection of MII oocytes and cumulus cells

In order to induce ovulation and collect as many MII oocytes as possible mice were superovulated. To superovulate the mice, females between four and six weeks old received an i.p injection of 5IU PMSG to stimulate follicle maturation. 48 hours after the injection of PMSG the mice were i.p injected with 100µl of 5IU human chorionic gonadotropin (hCG, Sigma, C1063) in order to induce ovulation. 14 hours after the injection of hCG the mice were sacrificed and the ovaries with the oviducts were removed and placed in prewarmed M2 medium with N-2-hydroxyethylpiperazine-N-2-ethane sulfonic acid (HEPES; Sigma, M7167-50ML). The oviduct was then torn open using forceps, allowing the release of the cumulus-oocyte-complexes

(COCs). Using a pipette, the COCs were moved from the M2 medium into a drop of 8IU/µl hyaluronidase (Sigma, H3506-100MG) that had been diluted 1000X in the M2 medium. The COCs were then incubated at 37°C for five minutes. Following incubation, the oocytes were moved into drops of warmed medium and washed to remove CCs. If any CCs remained the process was repeated with a new drop of hyaluronidase until the oocytes were clean. The ovulated oocytes were then collected in minimal media and stored at -80°C. Ovulation was also induced in mice over 40 weeks of age, in this case, 7IU of PMSG and hCG was used rather than 5IU.

To collect the CCs, the removed cells were collected from the drop of hyaluronidase using a pipette into a tube kept on ice. The cells were spun in a centrifuge at 2000rpm for ten minutes at 4°C. Following the first centrifugation, the supernatant was removed, and the cells were washed with 100µl of cold PBS. The cells were centrifuged one more time and the supernatant was removed. The collected CCs were frozen on dry ice and stored at -80°C.

2.4. Granulosa Cell Collection Protocol

In order to collect GCs, females received an i.p injection of 5IU PMSG and were sacrificed 46 hours following the injection. The ovaries were removed and placed into cold PBS to be cleaned and have their fat removed, being careful not to puncture the ovary in the process. Once the fat was removed the ovaries were placed in a small amount of cold PBS and punctured with a 30G needle to release the GCs. The cells were collected using a pipette into a 1.5ml tube being kept on ice. Following collection, the cells were centrifuged at 2000rpm for ten minutes at 4°C. After the first spin, the supernatant was removed, and the cells were washed with 100µl of

cold PBS. The cells were centrifuged once more, and the supernatant was removed before the cells were frozen on dry ice and stored at -80°C.

2.5. Conventional PCR, RT-PCR, and RT-qPCR

All primers used were purchased from Sigma and kept at -20℃ in a stock concentration of 100µM.

Table 2. Summary of *Odc* primers

#	Name	Sequence	Tm (℃)	Location
F0	Original F	ATTGTTCACTGAGTTTGAGTGC	61.6	Intron 1
F1	New Odc forward-1	GGATATTAGAAGGCATTTGAGG	63.0	Intron 1
F3	odc-RTB-F	CGTGCTCGGCGTATAAGTAG	63.8	Exon 1
F5	odc-RTB-F5	CACCACTCCAAGAAGGCAG	62.9	Exon 2
R0	Original R	TGTGTCTCAGAAGCATATCTGC		flox
R1	New Odc R	CATAGAACGCATCCTTATCGTC	64.3	Exon 4
R2	odc-RTB-R	CGCAACATAGAACGCATCC	64.4	Exon 4

Table 3. Summary of Cre-Recombinase and control primers used

#	Name	Sequence	Tm (℃)
Gdf9-F	gdf9-iCre-F1	GCAGTAAGCCATCAGTTATTCT	61.6
Gdf9-R	gdf9-iCre-R1	GGTAGTCCCTCACATCCTCA	61.2
Cyp19-F	Cre-Cyp19F	ACTTGGTCAAAGTCAGTGCG	60

Cyp19-R	Cre-Cyp19R	CCTGGTGCAAGCTGAACAAC	62
Actin-F	Mouse β-actin F	CCAGAGCAAGAGAGGTATCC	62
Actin-R	Mouse β-actin R	CTGTGGTGGTGAAGCTGTAG	62

2.5.1. DNA Extraction and Conventional PCR

Conventional PCR and DNA extraction were done using the KAPA HotStart Mouse Genotyping Kit (Sigma, KK7352) with mouse ear tissue. Mice were genotyped for *Odc* using two combinations of primers. The first forward and reverse primers, labelled F0 and R0, were designed by Hardbower *et al* and put in the intron 5' to exon 2 on either side of the first loxP site (Fig. 3) [14]. These primers gave a wild-type *Odc* band at 228bp and an Odc^{Flox} band at 332bp. This combination was used for mice that had either Odc^{WT} or Odc^{Flox} as it could show whether or not the *Odc* gene had the additional loxP sequence. The second combination still used F0 but instead used a reverse primer at beginning of exon 4. The new reverse primer was labelled R1. This combination was used to show the presence of *Odc* which had exons 2 and 3 deleted. These primers gave a wild-type band at 1018bp, an Odc^{Flox} band at 1122bp, and an *Odc* deletion band around 300bp. Only one set of *GDF9-iCre* and *Cyp19-iCre* primers were used (Table 2). Our *GDF9-iCre* primers produced a band at 732bp while the primers for *Cyp19-iCre* produced a band at 290bp. Genotyping primers were used at a stock concentration of 10µM, with a working concentration of 0.5µM.

2.5.2. RNA Extraction and RT-PCR

RT-PCR was done to see if *Cyp19-iCre* or *GDF9-iCre* were able to successfully delete exons 2 and 3 of *Odc* in the oocytes or GC. This was done using pools of collected GVBD oocytes or GCs taken from WT and *Odc*-KO females, as well as the liver to act as a positive control. RNA extraction of GC and oocytes was done using the Arcturus PicoPure RNA Isolation Kit (Applied Biosystems, 12204-01), and RNA extraction of the liver was done using TRIzol Reagent (Invitrogen, 15596-026). The extracted RNA was quantified using NanoDrop™ One/OneC Microvolume UV-Vis Spectrophotometer (ThermoFisher Scientific, ND-ONE-W). RT-PCR was done using the OneStep RT-PCR Kit (Qiagen, cat. 210210). Primers were designed in order to see an intact copy of *Odc* and a truncated copy that had exons 2 and 3 deleted in the mRNA. For this, primers F3 and R2 were used (Table 2). They showed a WT band at 484bp and a truncated band at 268bp. F3 was located at the beginning of exon 1 and R2 was located at the beginning of exon 4 (Fig. 3). Additionally, *β-actin* was used as an internal control, using primers designed by Hardbower *et al* (Table 3). *β-actin* produced a PCR product of 436bp. All of the primers were used at a stock concentration of 10µM with a final concentration of 0.6µM.

2.5.3. cDNA Synthesis and RT-qPCR

RT-qPCR was done in order to quantify *Odc mRNA* expression in the GC of WT mice versus GC-specific *Odc*-KO mice. This was done using the Powerup SYBR Green Master Mix (Applied Biosystems, A25741) with cDNA synthesized from total GC RNA. cDNA was made using the SuperScript IV First-Strand Synthesis System (Invitrogen, 18091050). For RT-qPCR, a forward primer labelled F5 was used in combination with R2 (Table 1). F5 was located in exon 2 (Fig. 3). With the forward primer in this location cells that contained Odc^{WT} would produce a

product of 237bp, but those that had the exons successfully deleted would not produce a PCR product. *β-actin* was once again used as an internal control, producing a band at 436bp. RT-qPCR was done in duplicate with every reaction containing 1.5ng/µl of GC RNA. The RT-qPCR primers were used at a stock concentration of 1µM with a final concentration of 200nM. RT-qPCR was carried out using the 7500 Fast Real-Time PCR system (Applied Biosystems, 4377355).

2.6. Western Blot Protocol

ODC protein was detected via western blot using a monoclonal mouse antibody (Origene, TA501546). GAPDH was used as a control and detected also using a monoclonal mouse antibody (ThermoFisher Scientific**,** AM4300). Protein extraction was done using RIPA buffer with a protease inhibitor cocktail plus Laemmli sample buffer (Sigma, S3401-10VL). RIPA buffer comprised of 50mM Tris HCl (pH 8.0), 150 mM NaCl, 1% Triton X-100, 0.5% sodium deoxycholate, 0.1% sodium dodecyl sulfate (SDS), and fresh protease inhibitor (1 tablet/10mL).

Oocytes and GC were collected as indicated above. To increase ODC protein content in mouse oocytes, GV oocytes were incubated for five hours at 37°C in a drop of M2 medium to GVBD in the presence of 100µM of the 20S proteasome inhibitor MG-115 covered in mineral oil [37,38]. 100µM MG-115 was prepared from 50mM stock in dimethyl sulfoxide (DMSO) by adding 1µl of stock solution to 500µl of M2 medium. Following incubation, the oocytes were washed in warm PBS and collected into a 1.5ml microcentrifuge tube and frozen on dry ice. Oocytes were found to yield an ODC signal at a concentration of 100 oocytes, as such oocytes were collected and frozen in groups of 100. To extract proteins from oocytes and GC, 5µl of RIPA buffer and 15µl of 2X sample buffer were added to tubes containing collected oocytes and

GC and gently mixed. The tubes were boiled for five minutes and then left on ice until ready to use.

Ovary, liver, and brain tissue were used as positive controls for western blot experiments. Tissue was collected from the mice into a 1.5ml microcentrifuge tube and weighed before being frozen on dry ice. The tissue was homogenized with a disposable pestle before adding RIPA buffer (500µl/10mg) The tissue was then sonicated (Fisher, Sonic Dismembrator Model 300) at 30Hz in the RIPA buffer three times for thirty seconds each, keeping the samples on ice between each repeat. Following sonication, the samples were incubated on ice for thirty minutes and then centrifuged at 14 000rpm at 4℃ for 15 minutes. Once centrifugation was complete the supernatant, now the tissue extract, was taken to a new tube. 50µl of this tissue extract was mixed with 50µl of 2x Laemmli sample buffer and boiled for five minutes. Following boiling, the samples were kept on ice until ready to use or stored in the -80℃ freezer.

Western blot was done using a 10% sodium dodecyl-sulfate polyacrylamide gel electrophoresis (SDS-PAGE) gel and transferred to a nitrocellulose membrane. Following the transfer, the nitrocellulose membrane was blocked in a solution of 5% milk in tris-buffered saline with tween (TBST) for at least an hour at room temperature. TBST contained 1M Tris (pH 7.5), 5M NaCl, Tween 20, and ddH_2O. After blocking, the membrane was put into a sealed bag containing the primary antibody. The ODC antibody was used at concentrations of 1:300 or 1:1000, and the GAPDH antibody was used at concentrations of 1:1500 or 1:3000 in the blocking solution. The membrane with the primary antibody was stored at 4℃ for incubation at least overnight.

Following primary antibody incubation, the nitrocellulose membrane was washed three times in TBST at room temperature for 15 minutes. After the wash, the nitrocellulose membrane was

put in a 3000X donkey anti-mouse IgG secondary antibody (Sigma, AP192P) in the blocking solution for one hour at room temperature. Following secondary antibody incubation, the nitrocellulose membrane was washed three times in TBST for 15 minutes each at room temperature. The protein signal was detected via electrochemiluminescence reaction (ThermoFisher Scientific, 34580) and pictured using the ChemiDoc MP Imaging System (Bio-Rad, 17001402).

2.7. Follicle Counting Protocol

Follicle counting was done to see if knocking out *Odc* in the oocyte affected follicle maturation. This was first done using three eight-week-old oocyte-specific *Odc*-KO females and three eight-week-old WT females. All six of these mice were first i.p injected with 5IU PMSG followed by 5IU hCG 48 hours later and were sacrificed five hours post-hCG injection. Follicle counting was also done using ovaries taken from 42-44-week-old mice. These older mice were superovulated following the superovulation protocol stated previously and the released MII oocytes were collected from the oviduct and, separately, the ovaries were fixed for follicle counting. For these older mice, both ovaries were taken for follicle counting. Ovaries for follicle counting were fixed for 24 hours in 10% formalin (Sigma, HT501128-4L) at 4°C, before they were washed three times for five minutes each in PBS, followed by three times for five minutes each in 70% ethanol. The ovaries were kept in 70% ethanol at room temperature until they were sent away for paraffin embedding. They were then embedded in paraffin and cut into 5µm sections by Dr. Mahdi Mohaqiq (a postdoc in the lab). For follicle counting, the whole ovary was sectioned.

Hematoxylin and eosin (H&E) staining of the eight-week-old ovary sections was done by honours student Nichole Dai, and the staining of the 42–44-week-old ovaries was done by Dr. Mahdi Mohaqiq. Sections first underwent two 15-minute xylene washes (Fisher Scientific. X3P-1GAL), followed by three minutes washes in decreasing concentrations of ethanol (100%, 90%, 80%, and finally 70%), and then briefly washed in distilled water. Sections were then stained in hematoxylin solution (Sigma, HHS16-500ML) for three minutes and dipped in distilled water 1-three times. After hematoxylin staining, the sections were put into 1% acid alcohol solution (Sigma, A3179-1L)) for 30 seconds and then bluing buffer (Epredia, 7301) for 60 seconds. The sections were once again dipped in distilled water followed by three minutes washed in 70% and then 80% ethanol. They were then moved into eosin solution (Sigma, 1.09844.100) for nine minutes. Following eosin staining sections were washed for one minute in 90% ethanol, and then two times for one minute each in 100% ethanol. Finally, the sections were washed in xylene for two hours and then mounted with a cover slip. When staining was finished slides were coded by Dr. Mahdi Mohaqiq for follicle counting by me. Follicle counting and imaging were done using the EVOS™ FL Auto 2 Imaging System (Invitrogen, AMAFD2000) and follicles were classified according to Pedersen and Peters method (Fig. 6) [29].

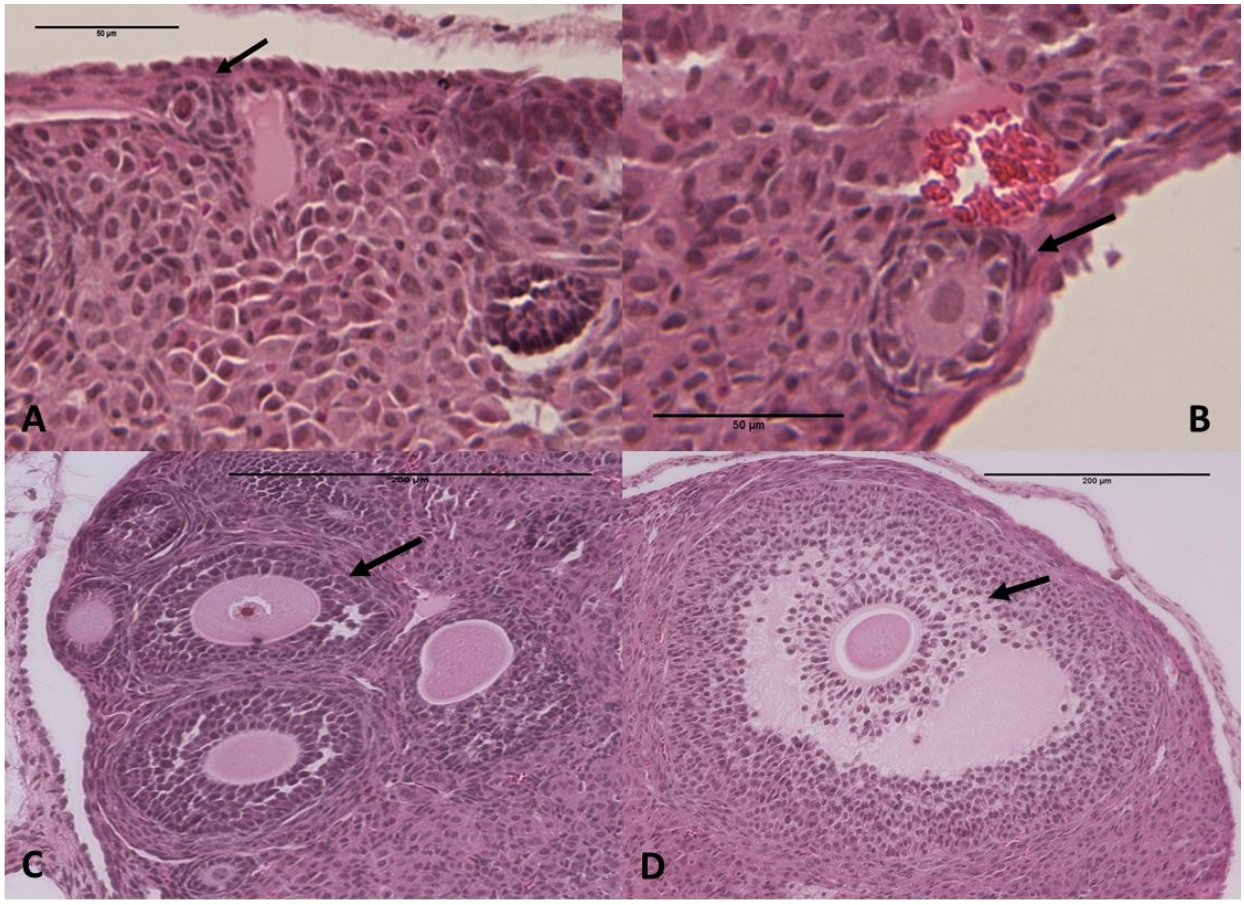

Figure 6. The four classes of follicles based on Pedersen and Peters method of classification.
Figure showing the four classifications of follicles; primordial (A), primary (B), secondary (C), and antral (D).

2.8. Cell Sorting Protocol

To determine cell cycle stages, collected granulosa cells were stained with propidium iodide (PI) before being subjected to fluorescence-activated cell sorting (FACS). One drawback of only using PI is that it cannot distinguish between the G2 phase and the M phase. Anti-MPM2, a monoclonal antibody used to determine if a cell is in M-phase by binding to mitosis-specific protein MPM2, was tried alongside the PI staining. However, we were unable to get a consistent signal and were therefore unable to get any data for the proportion of cells in the M-phase.

For FACS analyses, GC were collected into a tube in minimal medium and spun at 2000rpm for ten minutes at 4°C. Following centrifugation, the supernatant was removed, being careful not to disturb the pellet. The pellet was then washed in 100µl of PBS and spun once more in the same conditions. After the second spin 50µl of supernatant was removed and the GC were mixed gently to resuspend the cells. 500µl of cold 70% ethanol (stored in a -20°C freezer) was then slowly added to the tube one drop at a time. The cells were then incubated on ice for one hour. Following the one-hour incubation, the cells were spun at 2000rpm for ten minutes at 4°C and the supernatant was removed, once again being careful not to get too close to the pellet. The GC were then washed three times for five minutes each in 0.3% bovine serum albumin (BSA) in PBS. In between each wash, the cells were spun at 2000rpm for ten minutes and the supernatant was removed. Once the three washes were complete 200µl of 0.3% BSA in PBS with an additional 5µl of PI was added to the tube and mixed via pipette. This was then left to incubate overnight at 4°C. Cell sorting was done using the BD LSR Fortessa™ Cell Analyzer (BD Biosciences) which was operated by Mr. Fernando Ortiz from the Flow Cytometry and Cell Sorting Core Facility.

2.9. Fertility Evaluation

The fertility of the oocyte and GC-specific *Odc*-KO mice was evaluated via breeding. KO females and $Odc^{Fl/Fl}$ control sisters were paired with male littermates or with wild-type (WT) BDF1 males purchased from Charles River, as specified below. As pups were born the litter size and birth weight was recorded to see if the knockout caused any changes in the size or health of the litter.

The first fertility experiment was done using two *Odc*$^{Fl/-}$*; GDF9-iCre* females and two *Odc*$^{Fl/Fl}$ controls paired with male littermates. These mice were in breeding from March 21st, 2021, until July 2nd, 2021, when one KO and one control pair were mistakenly euthanized.

The second fertility experiment was done using five *Odc*$^{Fl/Fl}$*; GDF9-iCre* females and five *Odc*$^{Fl/Fl}$ controls paired with WT BDF1 males purchased from Charles River. These mice were put into breeding when they were between eight and ten weeks old on Oct 23rd, 2021, until the males were removed on March 21st, 2022, when the females were between 29 and 31 weeks old. While in breeding one knockout female had to be euthanized due to dystocia at 17 weeks old, one control female had to be euthanized due to rectal prolapse at 16 weeks old, and an additional control female had to be euthanized due to uterine prolapse at 26 weeks old. In order to keep the breeding consistent these females were not replaced, and the breeding carried on with four oocyte-KO pairs to three control pairs.

Two *Odc*$^{Fl/Fl}$*; Cyp19-iCre* females and two *Odc*$^{Fl/Fl}$ control sisters were put into breeding at eight weeks old with male *Odc*$^{Fl/Fl}$ littermates on March 22nd, 2022. Active breeding was stopped on Nov 24th, 2022, when the males were removed. During breeding one KO pair has been euthanized due to mastitis at 30 weeks old, leaving one GC-specific *Odc*-KO pair to two control pairs. Three *Odc*$^{Fl/-}$*; Cyp19-iCre* females and three *Odc*$^{Fl/Fl}$ control sisters were put into breeding between June 24th and July 12th, 2022, and were taken out of breeding on Nov 24th, 2022. Of these six pairs, one of the control pairs died in labour leaving three KO pairs against two control pairs. Additionally, we were able to breed *Odc*$^{Fl/-}$*; Cyp19-iCre; GDF9-iCre* double-KO mice. Two of these oocyte and GC-specific *Odc*-KOs were in breeding with *Odc*$^{Fl/Fl}$ males against two *Odc*$^{Fl/Fl}$ controls. However, one of these control pairs died in labour, leaving two KO

pairs against one control pair. Breeding pairs for the oocyte and GC-specific *Odc*-KO were separated on Nov 24th, 2022.

2.10. Statistical Analysis

All statistical analysis was performed using GraphPad Prism 9.4.1, with test details in figure legends. Western blot quantitative analysis was done using Fiji-ImageJ.

3. Results

3.1. Oocyte-Specific *Odc*-KO

3.1.1 Oocyte-Specific *Odc*-KO Genotyping

In order to see if the mice had inherited the floxed copy of *Odc*, as well as *GDF9-iCre*, PCR-genotyping was done using ear tissue taken at three weeks old when the mice were weaned. The *Odc* primers determined if the mouse carried a WT copy of *Odc* (Odc^{WT}), a floxed copy (Odc^{Fl}), or a copy that already had exons 2 and 3 looped out (Odc^{-}). The primers used only to show the presence of either a WT copy or a floxed copy of *Odc* were labelled F0 and R0 and produced a PCR product of 228bp for a WT copy and 332bp for a floxed copy (Fig. 7). A different reverse primer labelled R1 was used with F0 to determine if the mice carried an already deleted copy of *Odc,* these primers produced a product of 1018bp for Odc^{WT}, 1122bp for Odc^{Fl}, and a band around 300bp for Odc^{-} (Fig. 8). For *GDF9-iCre* primers that created a PCR product of 732bp were used (Fig. 7 and 8). Mice that were confirmed to be homozygous for Odc^{Fl} or carried Odc^{Fl} in the background of heterozygous *Odc* ($Odc^{Fl/-}$), alongside *GDF9-iCre*, were then used for experiments.

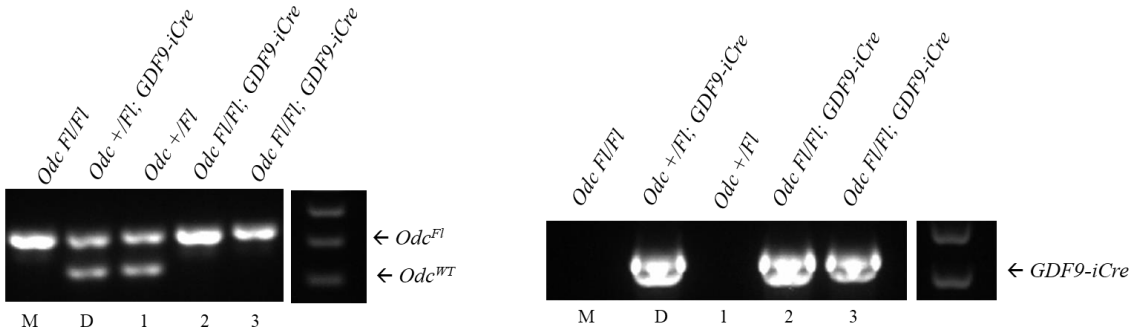

Figure 7. Genotyping of oocyte-specific knockout pups using *GDF9-iCre* and *Odc*-specific primers
Genotyping results showing $Odc^{Fl/Fl}$; *GDF9-iCre* oocyte-specific knockout mice from mating a homozygous $Odc^{Fl/Fl}$ mother with an $Odc^{+/Fl}$; *GDF9-iCre* father. Results showing the presence of Cre-recombinase are on the right-hand-side with a positive band around 700bp. Results showing the presence of *Odc* are shown on the left-hand-side with the band indicating wild-type at 228bp and the band indicating Odc^{Fl} at 332bp

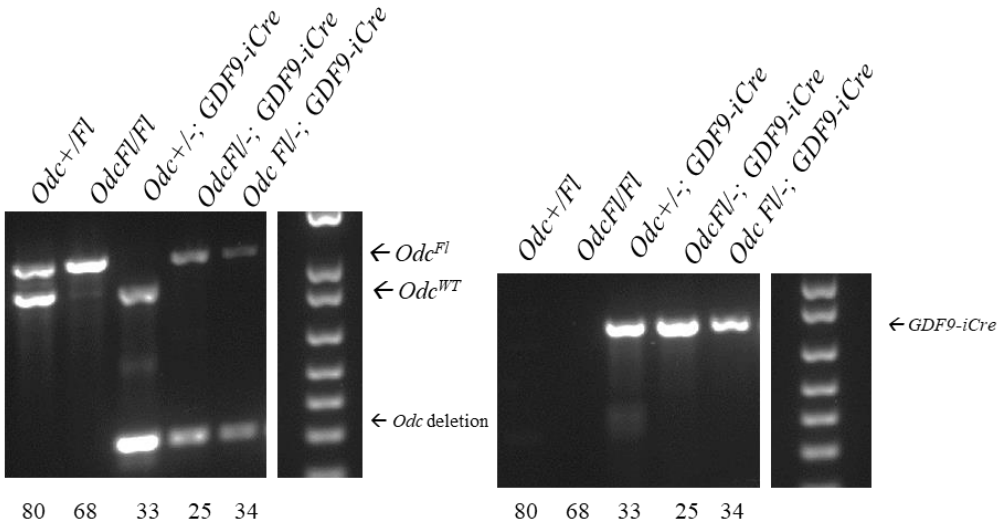

Figure 8. First oocyte-specific knockout mice with controls.
PCR results showing the genotypes of two oocyte-specific KO mice, numbers 25 and 34, versus three controls, numbers 80, 68, and 33. The band indicating Odc^{Fl} can be found around 1122bp, the Odc^{WT} band around 1018bp, the *Odc* deletion around 300bp and the band for *GDF9-iCre* at 723bp.

3.1.2 Oocyte-Specific *Odc*-KO RT-PCR

To determine if exons 2 and 3 were successfully deleted in the oocytes, RT-PCR was used. This was done using total RNA extracted from GV/GVBD oocytes collected from oocyte-specific *Odc*-KO females and WT controls. Liver tissue collected from the oocyte-specific *Odc*-KO mice was also used as a control to confirm that the KO only occurred in the oocytes. RT-PCR primers were designed to show an intact *Odc* band and a truncated KO band with the two exons deleted. *β-actin* was used as an internal control.

Results of RT-PCR using oocytes collected from an oocyte-specific *Odc*-KO mouse showed a clear truncated copy of *Odc*. In contrast, the oocytes collected from the WT mouse, as well as the liver tissue collected from the KO mouse showed a larger band which still had exons 2 and 3 (Fig. 9). This experiment was repeated two more times using different mice which

produced the same result. The results of RT-PCR showed that exons 2 and 3 had been excised in only the oocytes of *Odc*$^{Fl/Fl}$; *GDF9-iCre* females. With these results, we could be sure that the start codon of *Odc* was removed thus completely knocking out *Odc* in the oocytes.

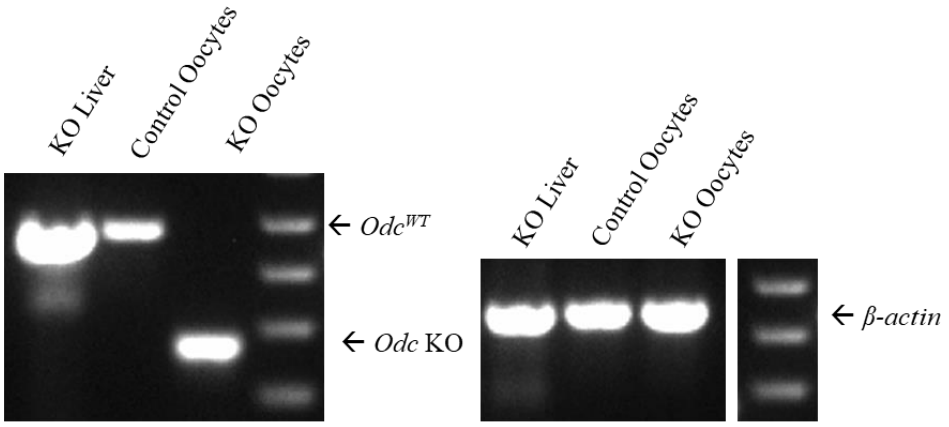

Figure 9. RT-PCR results using *Odc* (left) and *β-actin* (right) specific primers of *Odc*-KO oocytes versus control oocytes, as well as liver taken from the oocyte-specific *Odc*-KO mouse as a control

RT-PCR results of oocytes taken from an oocyte-specific *Odc*-KO mouse vs control oocytes, as well as liver control take from the *Odc*-KO mouse. Primers for *Odc* (left) were used to detect the presence of *Odc*-WT (484bp) and *Odc*-KO (268bp). Primers for *β-actin* (right; 436bp)) were used as controls. The presence of a deletion was detected in the KO oocytes while both the liver and control oocytes carried the WT copy, showing that the deletion had taken place

3.1.3 Oocyte-Specific *Odc*-KO Western Blot

Following the confirmation that *GDF9-iCre* had successfully looped out the start codon of *Odc*, we turned to western blot in order to confirm that *Odc* was no longer being translated. Western blot was done using an ODC-specific antibody on pools of collected GV/GVBD oocytes. The ODC antibody showed a band around 51kDa. GAPDH was used as an internal control, which showed a band around 37kDa. Based on our RT-PCR results we were expecting to see a decrease or a complete absence of ODC expression in the oocytes of the oocyte-specific *Odc*-KO mice.

Initially, we were unable to see a band for ODC using oocytes. However, ODC has one of the shortest half-lives of all the eukaryotic proteins [39], as such the proteasome inhibitor MG-115 was employed to prevent ODC degradation. Additionally, attempts at western blot showed that ODC produces three bands. Tissues such as the liver, ovaries, and granulosa cells produced three bands, while other tissues such as the brain produced only the upper band. With both of these factors in mind, 310 WT oocytes were collected and cultured at 37°C in the presence of 100μM MG-115 in M2 medium for five hours. This resulted in a strong upper ODC band in the oocyte lane (Fig. 10)

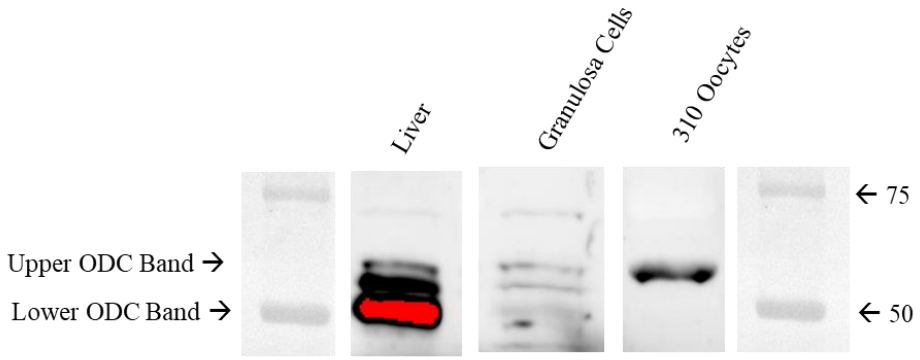

Figure 10. Western blot using 300X (2μl antibody in 1500ul blocking solution) ODC antibody showing a positive oocyte band, as well as the upper and lower ODC bands.
Western blot done using 310 oocytes cultured in MG-115, with liver, and granulosa cells being used as positive controls. Oocytes show a strong signal for the upper ODC band while the liver and granulosa cells show both upper and lower bands.

Due to having such a strong band using 310 MG-115 cultured oocytes, we theorized that 100 oocytes would also yield a band. We did western blot two more times, this time using 100 WT and 98 *Odc*-KO-oocytes that had been cultured in MG-115. Results showed a strong band in the WT-oocyte lane and a very faint band in the *Odc*-KO-oocyte lane. GAPDH confirms that this faint band was not due to a lack of protein in the sample. These results were expanded on with

quantitative analysis which showed that the *Odc*-KO oocytes did have a large reduction in ODC expression when compared to WT oocytes (Fig. 11).

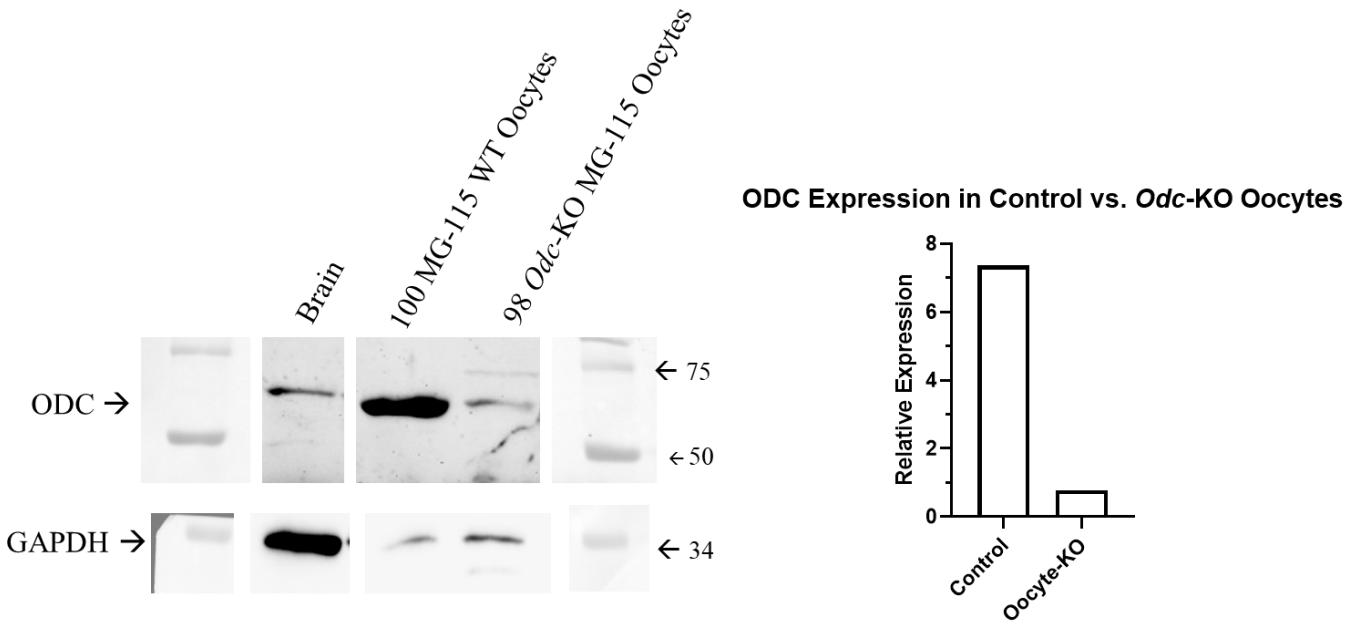

Figure 11. Western blot and quantitative analysis of 98 *Odc* knockout oocytes cultured in 100µM MG-115, vs 100 wild-type oocytes cultured in 100µM MG-115 with brain tissue being used as a control. Using 300X ODC and 1500X GAPDH specific antibodies (N=1).
Western blot done using 300X ODC (2µl antibody in 1500µl blocking solution) and 1500X GAPDH (1µl antibody in 1500µl blocking solution) antibodies against wild-type and *Odc* knockout oocytes that have been cultured in 100µM MG-115. Quantitative analysis showed a decrease of ODC expression in the *Odc*-KO oocytes. The ODC band can be found around 55kDa, while the GAPDH band can be found around 37kDa.

3.1.4 Follicle Counting of Oocyte-Specific *Odc*-KO Mice

As RT-PCR and Western blotting confirmed that *Odc* had been knocked out in the oocytes, follicle counting was done to see if this had any effect on oocyte and follicle development. The follicles were classed as primordial, primary, secondary, or antral, following Pedersen and Peter's classifications [29]. Slides were coded by Dr. Mahdi Mohaqiq, before handing them over for counting, and the codes were revealed only after counting. The entire ovary was sectioned at 5um thickness. Every tenth section was counted for a total of 20 sections

per ovary. For this experiment, three WT females and three oocyte-specific *Odc*-KO females were taken at eight weeks old. These mice were injected with both PMSG and hCG, and the mice were sacrificed five hours after the hCG injection. The counted follicles from each group were added together to get the average number of follicles in each stage for control and oocyte-specific *Odc*-KO mice. While the WT appeared to have a greater number of primordial, secondary, and total follicles, two-way ANOVA found no significant difference between any of the groups (P=0.1665; Fig. 12).

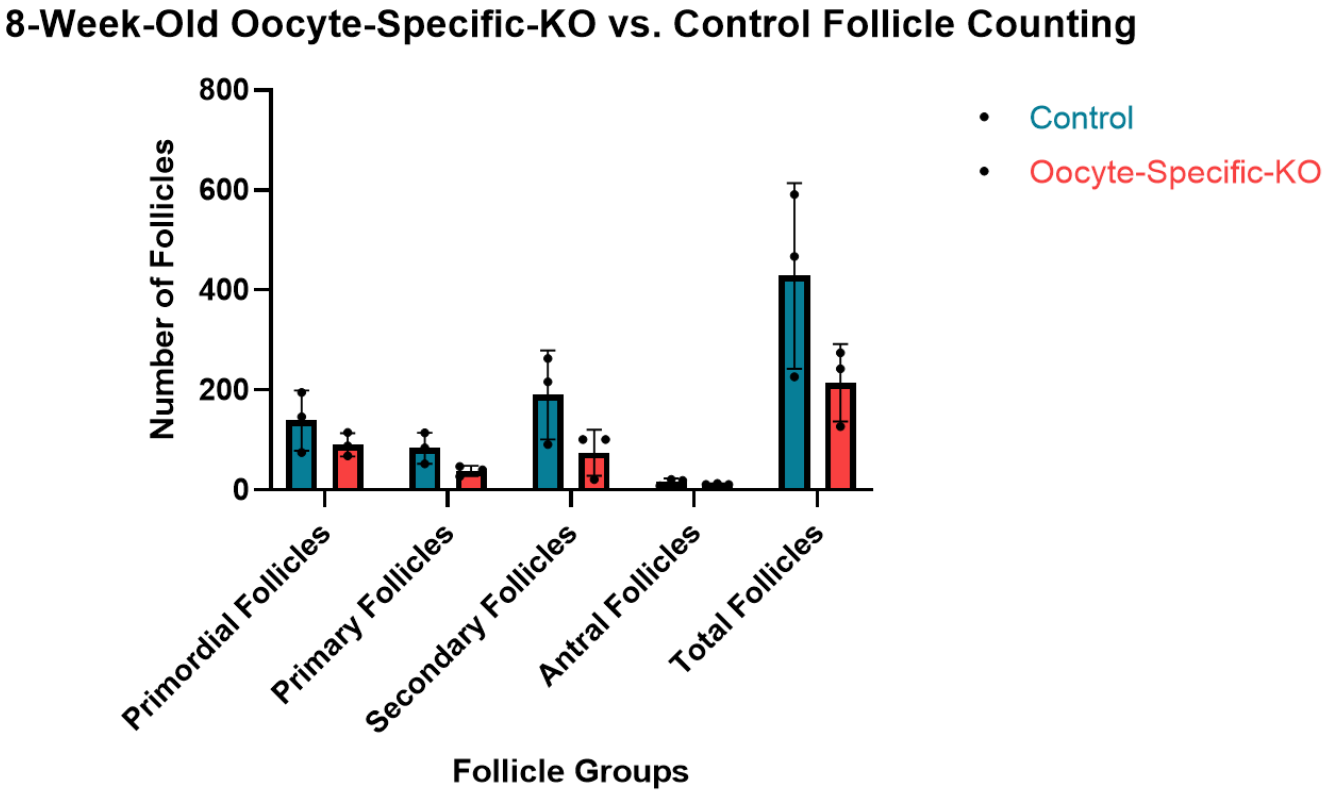

Figure 12. The difference in follicle number in eight-week-old control vs. oocyte-specific *Odc*-KO ovaries separated by the four major stages. (N=3)

Bar graph showing the average number of follicles counted in the ovaries taken from three eight-week-old oocyte-specific *Odc*-KO females and three eight-week-old control females separated by the four major growth stages. While there did appear to be a difference between the two groups in number of primordial, primary, and secondary follicles, Two-way ANOVA found no significant difference (P=0.1665).

That oocyte-specific *Odc*-KO did not affect follicle number was further supported by an experiment in which the follicle numbers of the two groups were compared in older mice (42-44 weeks). Unlike the experiment done with the eight-week-old mice, both ovaries were sectioned for this experiment resulting in approximately 50 sections per mouse, with every fifth section being taken for counting. These ovaries were collected 14 hours after the injection of hCG in order to collect ovulated oocytes from the oviducts. From this ovulation data, no difference was found between the number of ovulated oocytes in oocyte-specific *Odc*-KO mice versus WT controls (P=0.7226; Fig. 13). This was also reflected in the results of the follicle counting of the ovaries which also found no significant difference between the groups. Compared to the eight-week-old mice the 42-44-week-old mice were much closer in follicle number across all of the groups and two-way ANOVA found no significant difference (P=0.8640; Fig. 14). Due to these mice being super ovulated prior to follicle counting no antral follicles were present in either group.

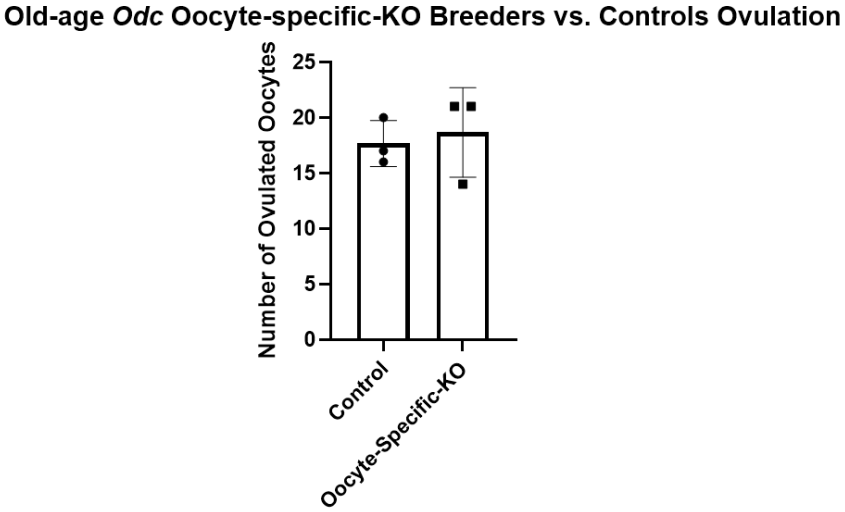

Figure 13. Average number of ovulated oocytes from 44-42-week-old oocyte-specific *Odc*-KO and control breeders. (N=3)
Average number of ovulated oocytes removed from the oviducts of three oocyte-specific *Odc*-KO breeders ages 43-42wks and three wild-type sisters ages 44-42wks. No difference was found between the two groups. A T-test found no significant difference between the groups (P=0.7226).

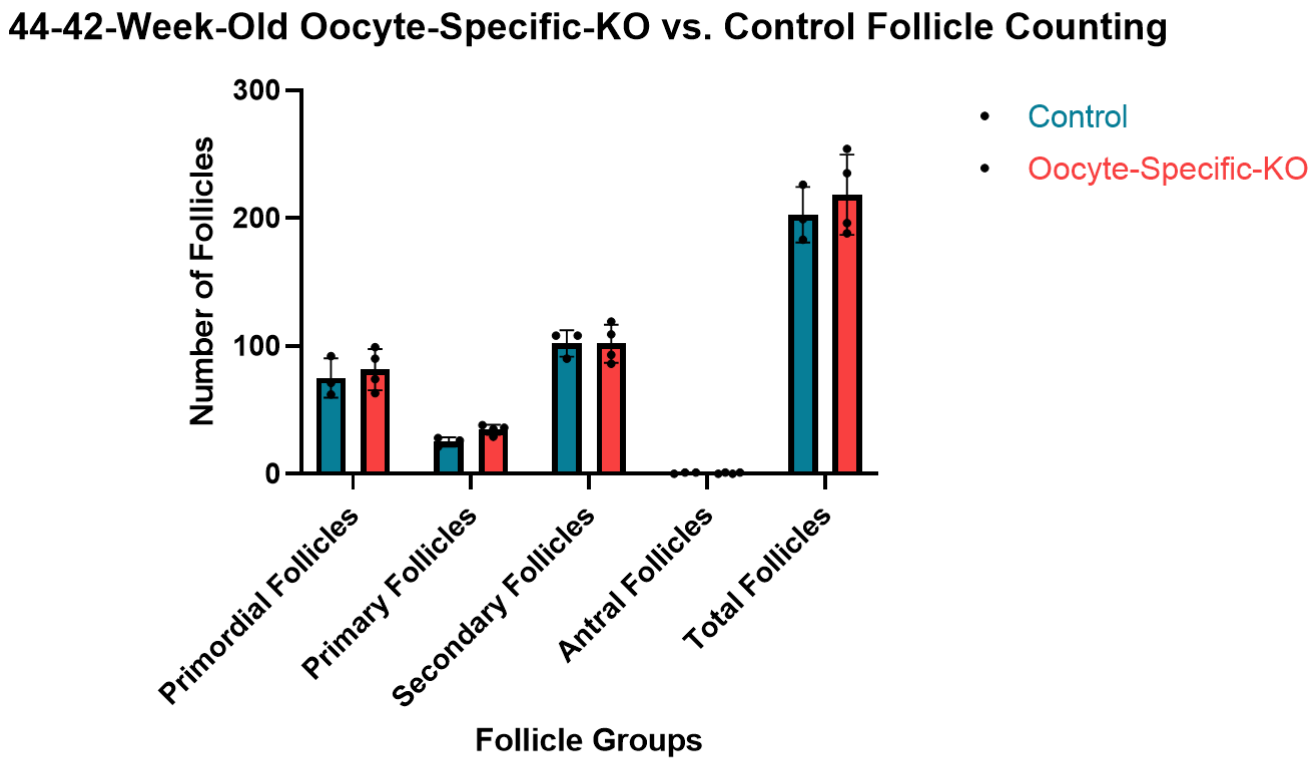

Figure 14. The difference in average follicle number in 44-42-week-old controls vs. oocyte-specific *Odc*-KO ovaries separated by the four major stages. (Control: N=3, KO: N=4)
Bar graph showing the average number of follicles counted in the ovaries taken from four 42-week-old oocyte-specific *Odc*-KO females and three 44-42-week-old control females separated by the four major growth stages. Two-way ANOVA found no significant difference between the groups (P=0.8640).

3.1.5. Oocyte-Specific *Odc*-KO Fertility Testing

To see if the deletion of *Odc* in the oocytes had any effect on the fertility of the mice, females that were confirmed to be oocyte-specific *Odc*-KOs via PCR-genotyping were put into breeding alongside $Odc^{Fl/Fl}$ control sisters. It had previously been found that mice that are older (≤8 months) experience a diminished rise in preovulatory ovarian ODC activity when compared to their younger counterparts. This activity decrease corresponds with the classic signs of reproductive aging, an increased rate of aneuploidies and miscarriage [37]. The oocyte-specific *Odc*-KO mice were put into continuous breeding for four or more months and were observed to

see if they experienced any reduced fertility compared to control littermates. The fertility of the mice was judged based on litter size. We also recorded the birth weight of the pups whenever possible.

3.1.5.1 Oocyte-Specific *Odc*-KO Short-Term Breeding

The first KO mice put into breeding were two $Odc^{Fl/Fl}$ control females, as well as two oocyte-specific *Odc*-KO females. These mice were paired with WT brothers. The oocyte-specific *Odc*-KO females had the genotype $Odc^{Fl/-}$*; GDF9-iCre*, making them an oocyte-specific *Odc*-KO in the background of full-body-heterozygous *Odc*. These pairs were in breeding for 15 weeks when a mistake led to KO pair 1 and control pair 1 being euthanized. During this time, all of the pairs were able to have at least three litters, with KO pair 2 being the exception having four litters. All KO female pregnancies progressed normally except for KO pair 2's first pregnancy which resulted in a premature stillbirth. However, she went on to have large healthy litters for all subsequent pregnancies. A students t-test found no significant difference when comparing the average number of pups born (P=0.5885; Fig. 15b).

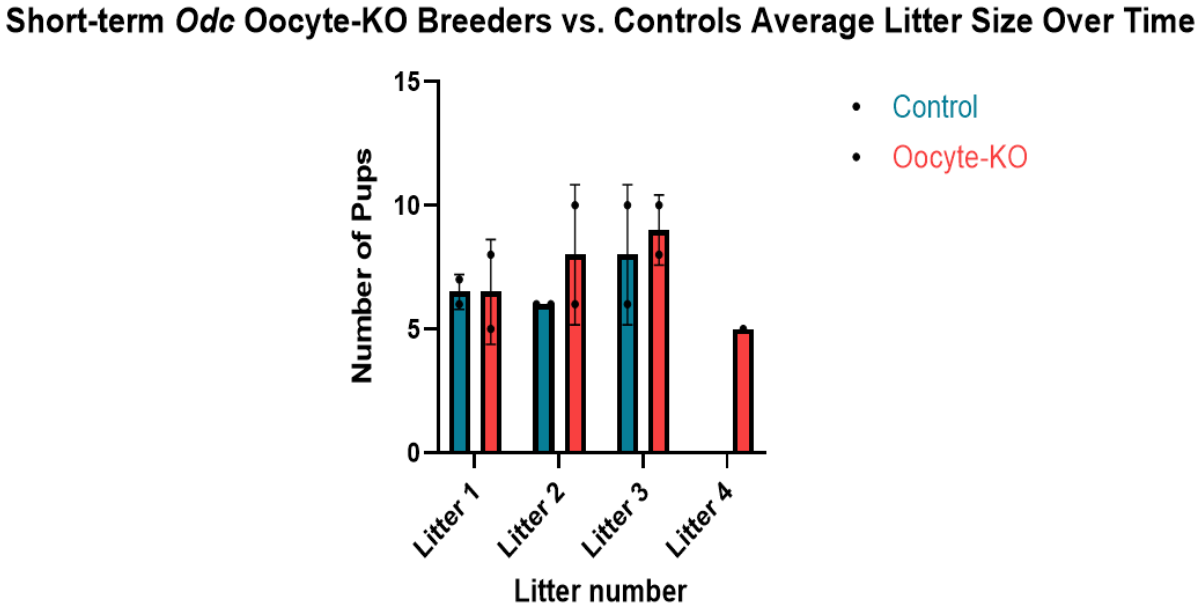

Figure 15a. The average litter size of control breeders vs. oocyte-specific *Odc*-KO breeders by litter number. (Control: N=6, KO: N=7)
Average litter size of two oocyte-specific *Odc*-KO females with the genotype $Odc^{Fl/-}$; *GDF9-iCre*, versus the average litter size of two wild-type sisters. Mice were in breeding from March 21st, 2021, to July 2nd, 2021, organized by litter number. In the three months the mice were in mating no significant difference was observed between control and KO litters.

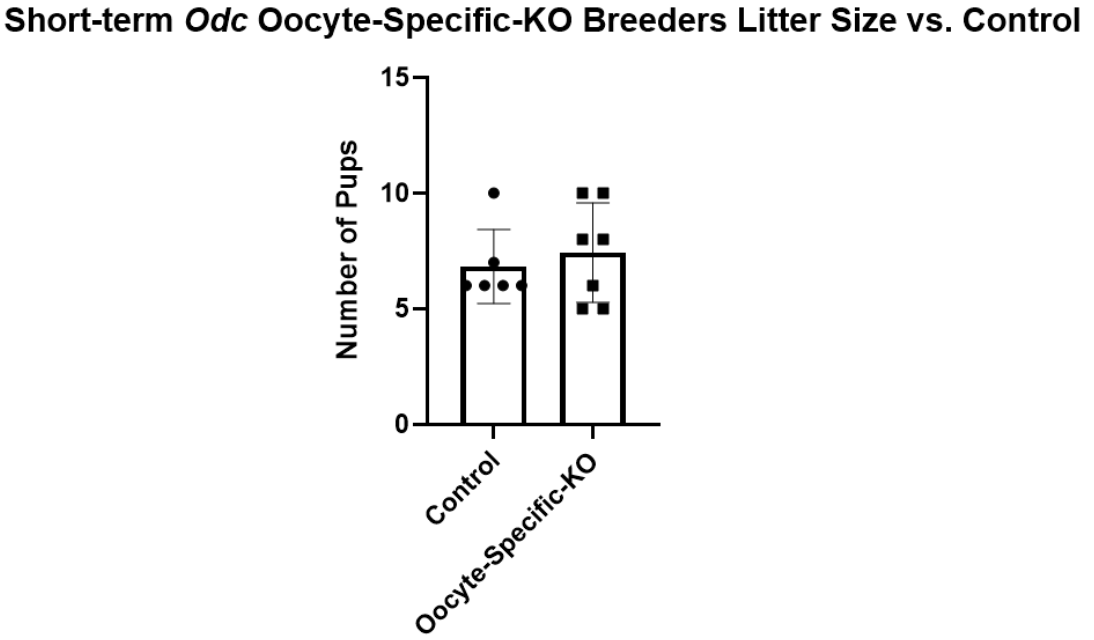

Figure 15b. Average litter size of control mice versus oocyte-specific *Odc*-KO in short-term breeding. (Control: N=6, KO: N=7)
Average litter size of two oocyte-specific *Odc*-KO females with the genotype $Odc^{Fl/-}$; *GDF9-iCre*, versus the average litter size of two wild-type sisters. Mice were in breeding from March 21st, 2021, to July 2nd, 2021. In the three months the mice were in mating no significant difference was observed between control and KO litters. A T-test found no significant difference between the groups (P=0.5885).

3.1.5.2 Oocyte-Specific *Odc*-KO Long-Term Breeding

For our second breeding experiment, we were able to obtain enough oocyte-specific *Odc*-KO mice to have five in breeding against five control sisters. These ten females were put into a long-term breeding experiment with BDF1 males purchased from Charles River. To confirm that the mice in breeding were indeed oocyte-specific knockouts, one pup from each pair was randomly selected for ear tip genotyping. If the mothers did indeed have *Odc* deleted in their oocytes, they would only be able to pass on a whole-body deletion to their pups as *Odc* has been altered in the gametes. Figure 16 shows the results of this genotyping. All pups from the KO pairings carried a full-body deletion, while the control pup, whose mothers did not carry *GDF9-iCre*, did not.

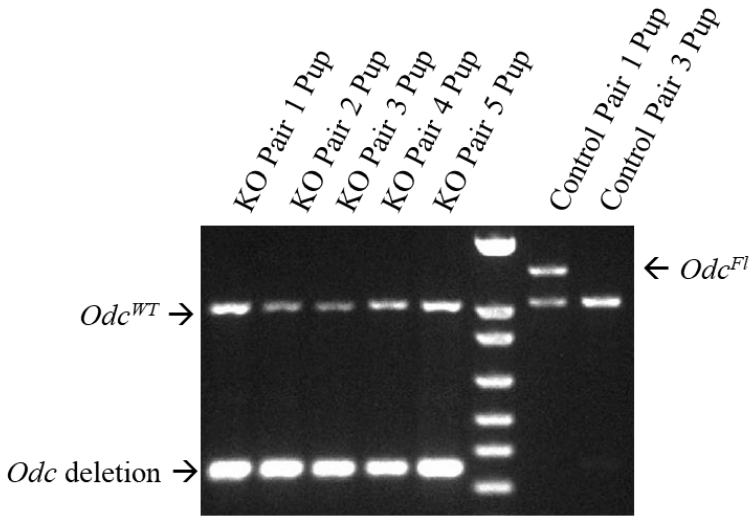

Figure 16. PCR results of mouse ear tips showing the presence of a whole-body deletion in the pups born from oocyte-specific *Odc*-KO moms.

PCR results of five pups born from oocyte-specific *Odc*-KO moms and two pups from control moms. Pups were randomly selected from each breeding pair. Presence of a whole-body deletion of *Odc* in pups shows that the mothers did have *Odc* deleted in the oocytes. Control pups did not inherit the deletion as their mother did not carry *GDF9-iCre*. The band indicating Odc^{Fl} can be found around 1122bp, the Odc^{WT} band around 1018bp, the *Odc* deletion around 300bp.

These mice stayed in mating until they were between 29 and 31 weeks old. With every new litter, the number of pups born was counted (Fig. 17a) and the birth weight was recorded whenever possible (Fig. 18). From the breeding data no significant difference was seen in the average number of pups born (P=0.9741; Fig 17b). Both groups had an average of eight pups per litter (Fig. 17b) that each weighed approximately 1.3g (Fig. 18), and both had between five to six litters during their 21 weeks of breeding with no significant gaps of time between pregnancies.

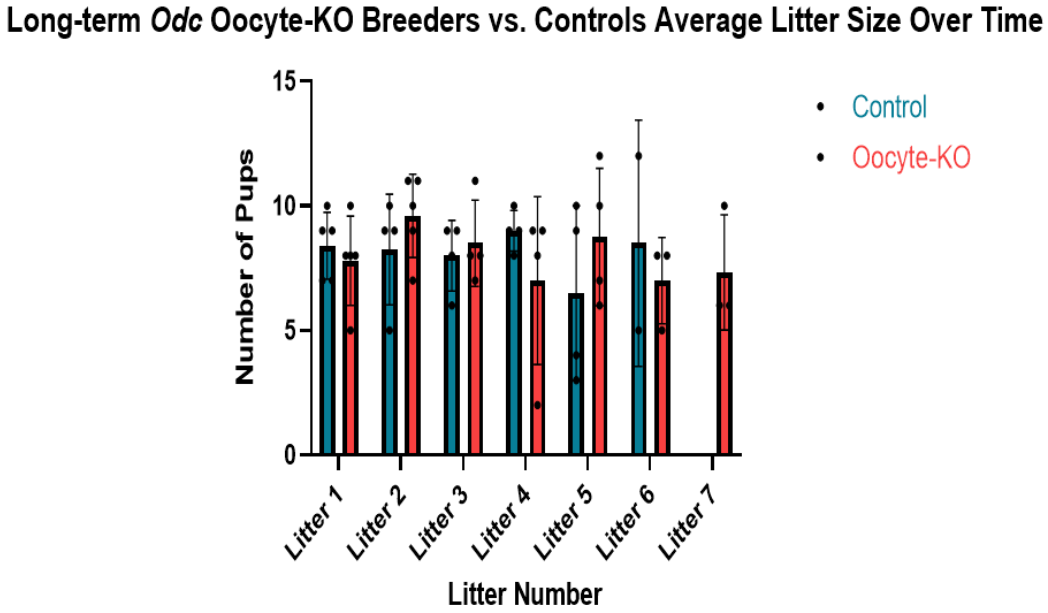

Figure 17a. Average litter size over time of control females versus oocyte-specific *Odc*-KO females in long-term breeding, organized by litter number. (Control: N=23, KO: N=28)
Average litter size of five oocyte-specific *Odc*-KO females with the genotype $Odc^{Fl/Fl}$; *GDF9-iCre*, versus the average litter size of five wild-type sisters. Mice were in breeding from October 23rd, 2021, to March 21st, 2022. No significant difference in litter size was observed.

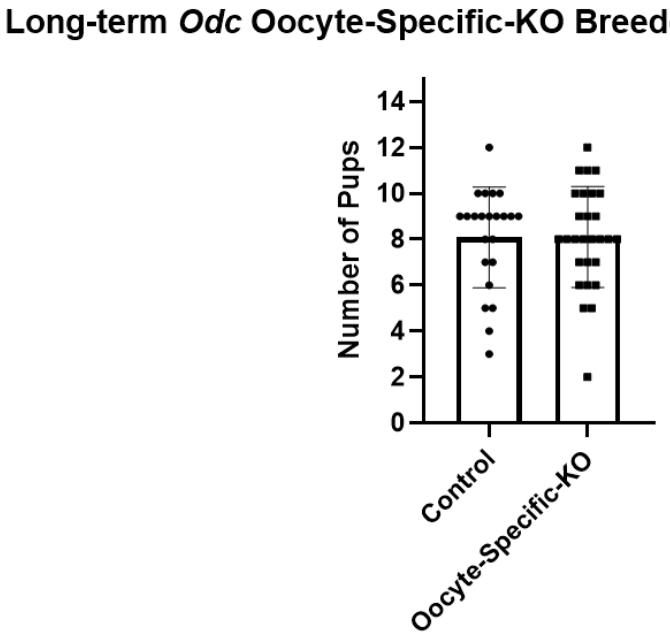

Figure 17b. Average litter size of control females versus oocyte-specific *Odc*-KO females in long-term breeding. (Control: N=23, KO: N=28)
Average litter size of five oocyte-specific *Odc*-KO females with the genotype $Odc^{Fl/Fl}$; *GDF9-iCre*, versus the average litter size of five wild-type sisters. Mice were in breeding from October 23rd, 2021, to March 21st, 2022. No significant difference in litter size was observed. A T-test found no significant difference between the groups (P=0.9741).

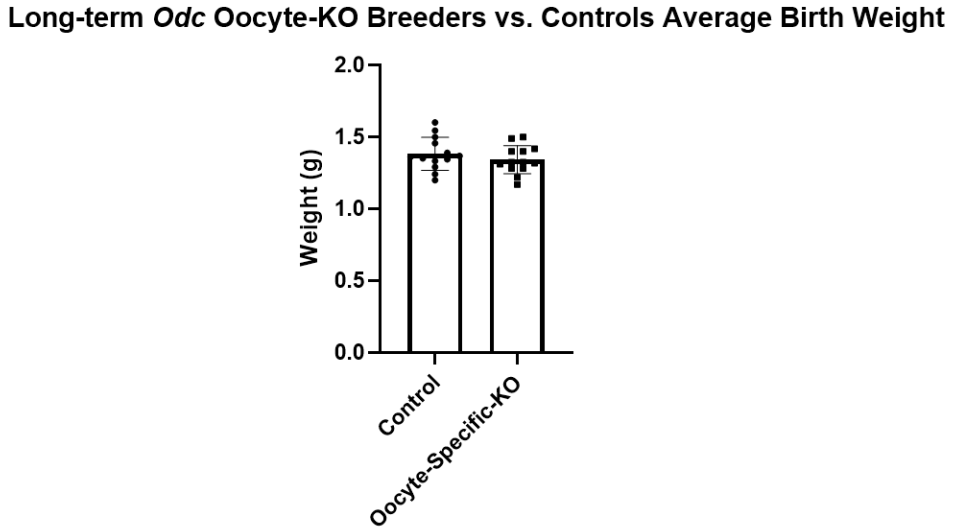

Figure 18. Average birth weight of control females versus oocyte-specific *Odc*-KO females in long-term breeding. (Control: N=13, KO: N=13)
Average birth weight of litters born to five oocyte-specific *Odc*-KO females with the genotype $Odc^{Fl/Fl}$; *GDF9-iCre*, versus the average birth weight of the litters of five wild-type sisters. Mice were in breeding from October 23rd, 2021, to March 21st, 2022. No significant difference in birthweight was found between control and oocyte-specific-KO pups. A T-test found no significant difference between the groups (P=0.3341).

3.2. Granulosa Cell-Specific *Odc*-KO

3.2.1 Granulosa Cell-Specific *Odc*-KO Genotyping

Just as in the oocyte-specific *Odc*-KO mice PCR-genotyping was done to identify GC-specific *Odc*-KO mice. In order to identify the presence of *Cyp19-iCre,* primers were designed that corresponded to the *Cyp19* promoter sequence and the Cre recombinase. This combination would amplify the *Cyp19-iCre* transgene and produce a PCR product of 290bp (Fig. 19 and 20). Mice with GC-specific *Odc*-KO in the background of heterozygous *Odc* were also identified (Fig. 20). The mice that were confirmed to be homozygous for Odc^{Fl}, or carried Odc^{Fl} in the background of heterozygous *Odc,* alongside *Cyp19-iCre,* were then used for experiments.

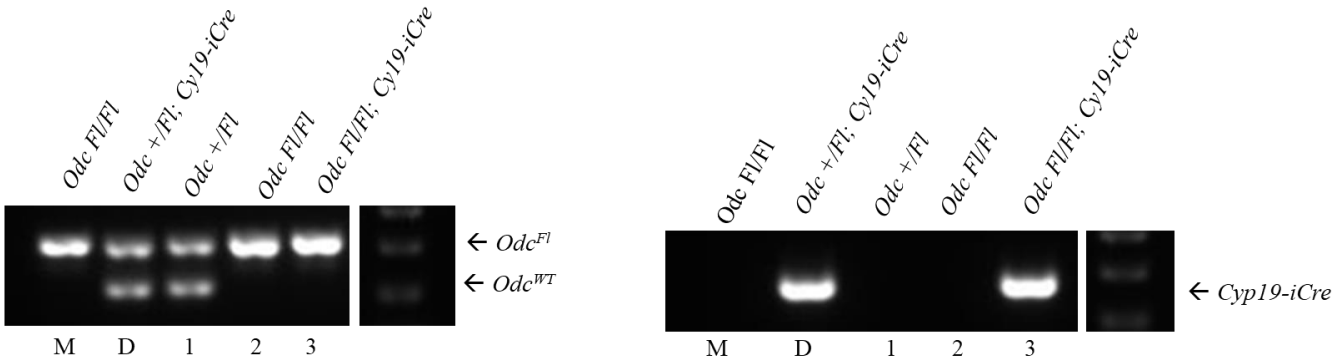

Figure 19. Genotyping of granulosa cell-specific *Odc*-knockout pups using *Cyp19-iCre* and *Odc*-specific primers

Genotyping results showing $Odc^{Fl/Fl}$; *Cyp19-iCre* granulosa cell-specific *Odc*-knockout mice from mating a homozygous $Odc^{Fl/Fl}$ mother with an $Odc^{+/Fl}$; *Cyp19-iCre* father. Results showing the presence of Cre-recombinase are on the right-hand-side with a positive band around 290bp. Results showing the presence of *Odc* are shown on the left-hand-side with the band indicating wild-type at 228bp and the band indicating Odc^{Fl} at 332bp

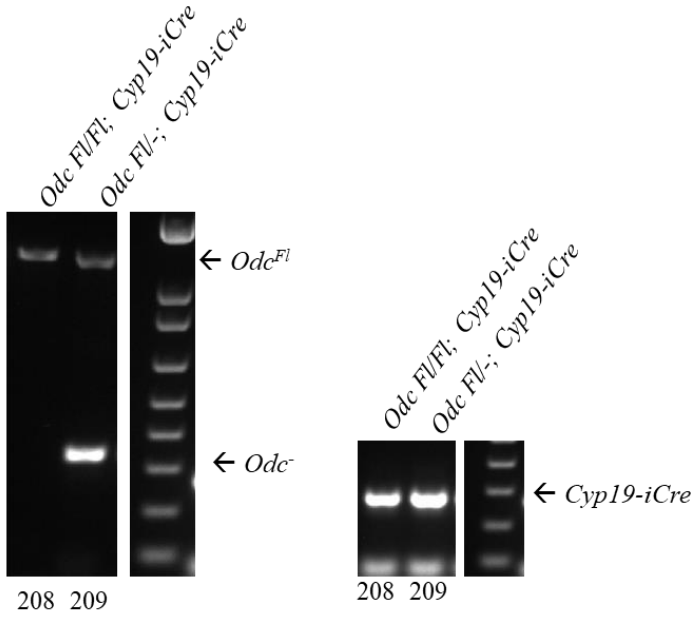

Figure 20. PCR of a granulosa cell-specific *Odc*-KO in the background of a full-body-KO and an $Odc^{+/Fl}$; *Cyp19-iCre* sister for comparison.

The band indicating Odc^{Fl} can be found around 1122bp, the Odc^{WT} band around 1018bp, the *Odc* deletion around 300bp. The band for *Cyp19-iCre* can be found at 290bp.

3.2.2 Granulosa Cell-Specific *Odc*-KO RT-PCR and RT-qPCR

RT-PCR was done using collected GC in order to determine if *Cyp19-iCre* had been successful in looping out exons 2 and 3. The same primers previously used with the oocytes were used once again, as well as primers for *β-actin* as a control. Unlike the oocytes that showed a clear deletion band with no trace of the WT band, granulosa cells taken from GC-specific *Odc*-KO mice showed both a WT and truncated *Odc* band (Fig. 21). This result indicated that *Cyp19-iCre* was not successful in deleting exons 2 and 3 in all of the granulosa cells. In order to better quantify the degree of the KO in the GC, RT-qPCR was used.

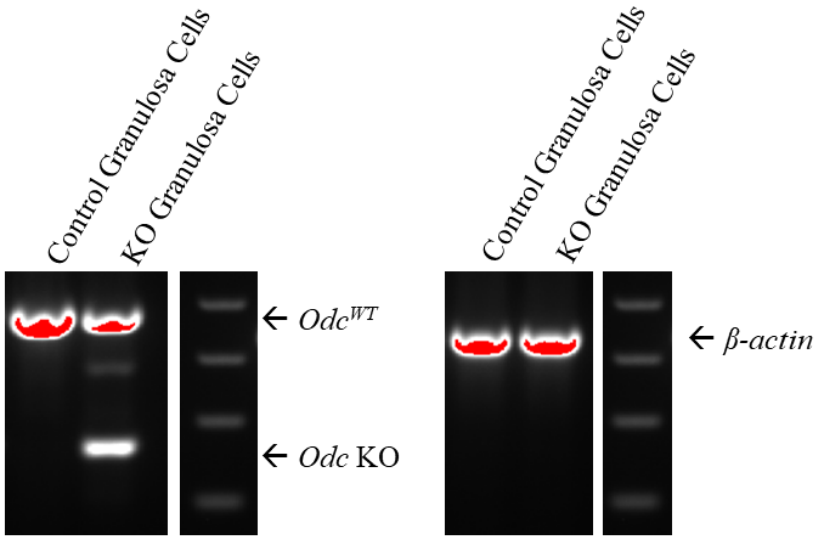

Figure 21. RT-PCR results of granulosa cells taken from wild-type and GC-specific *Odc*-KO females.
Figure showing the RT-PCR results from a GC-specific *Odc*-KO mouse and a control sister using granulosa cells taken from the ovary. Primers show the presence of *Odc*-WT (484bp) and *Odc*-KO (268bp). Granulosa cells collected from the KO mouse show both wild-type and KO bands, indicating a partial KO. In contrast the control cells only has a wild-type band.

RT-qPCR was done using a forward primer in exon 2 alongside the same reverse primer used for RT-PCR. With the forward primer in this location, cells which had exons 2 and 3 of *Odc* deleted would not produce a signal. *β-actin* was once again used as an internal control. While all

RT-qPCR trials using *Odc*$^{Fl/Fl}$*; Cyp19-iCre* granulosa cells showed a decrease in *Odc* mRNA expression, a t-test found no significant difference in the expression of *Odc* in control versus *Odc*-KO GC (P=0.4133). On average there appeared to be an approximately 35% drop in *Odc* expression in control versus *Odc*-KO cells taken from *Odc*$^{Fl/Fl}$*; Cyp19-iCre* mice (Fig. 22a).

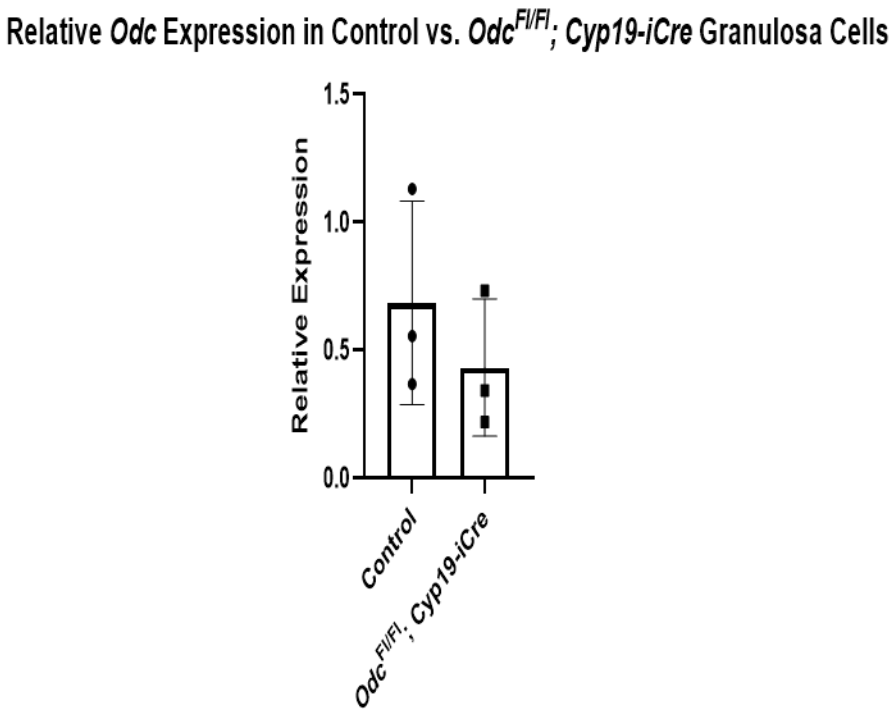

Figure 22a. Relative expression of *Odc* in control versus knockout granulosa cells (N=3)

Relative expression of *Odc* in granulosa cells taken from wild-type and GC-specific *Odc-KO* showing variability in the level of knockout. A T-test found no significant difference between the groups (P=0.4133).

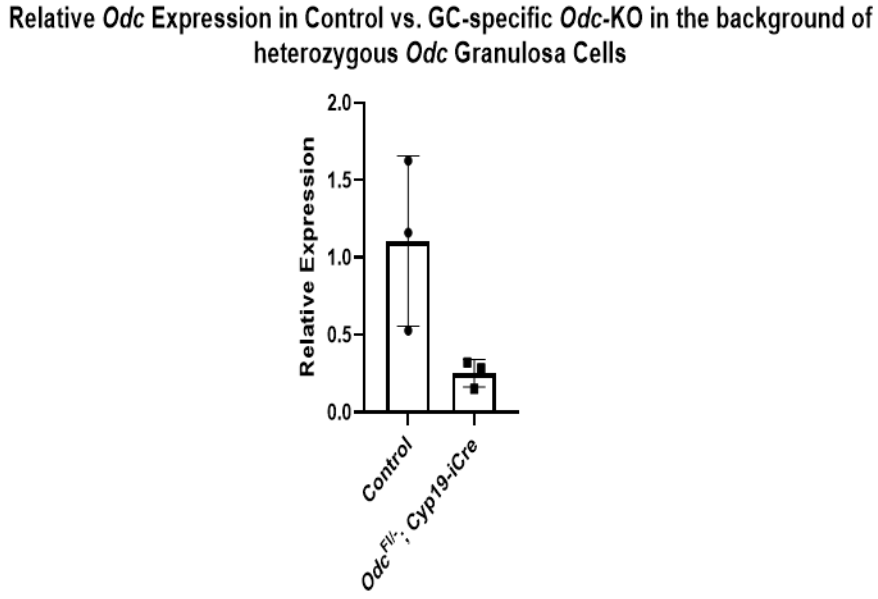

Figure 22b. Relative expression of *Odc* in control versus $Odc^{Fl/-}$ knockout granulosa cells (N=3)

Relative expression in wild-type granulosa cells versus granulosa cells taken from a GC-specific *Odc-KO* in the background of heterozygous *Odc* mouse, showing reduction of *Odc* expression in KO GC versus the control. A T-test found no significant difference between the groups (P=0.0571).

RT-qPCR was also done using GC taken from mice who had a granulosa cell-specific *Odc*-KO in the background of heterozygous *Odc*. This also did not result in a total KO of *Odc* in the GC. With these three trials of RT-qPCR using $Odc^{Fl/-}$; *Cyp19-iCre* GC, no significant difference was observed between the wild-type controls and the knockout GC (P=0.0571; Fig. 22b).

3.2.3 Granulosa Cell-Specific *Odc*-KO Western Blot

Western blot was done with the GC-specific *Odc*-KO mice three times. The first two trials were done using ovaries taken from GC-specific *Odc*-KO females and compared them against ovaries taken from a WT sister. The ovaries were used due to granulosa cells taking up a large portion of the ovary. It was thought that if *Odc* was deleted in the GC, then this could be reflected in the overall ODC signal of the ovaries. The last trial was done using granulosa cells directly. Figure 23 shows the results of these trials. Just as was the case with RT-qPCR there is a partial reduction in ODC expression. However, when comparing the GC-specific *Odc*-KO expression across all three trials no significant difference was found (P=0.3134).

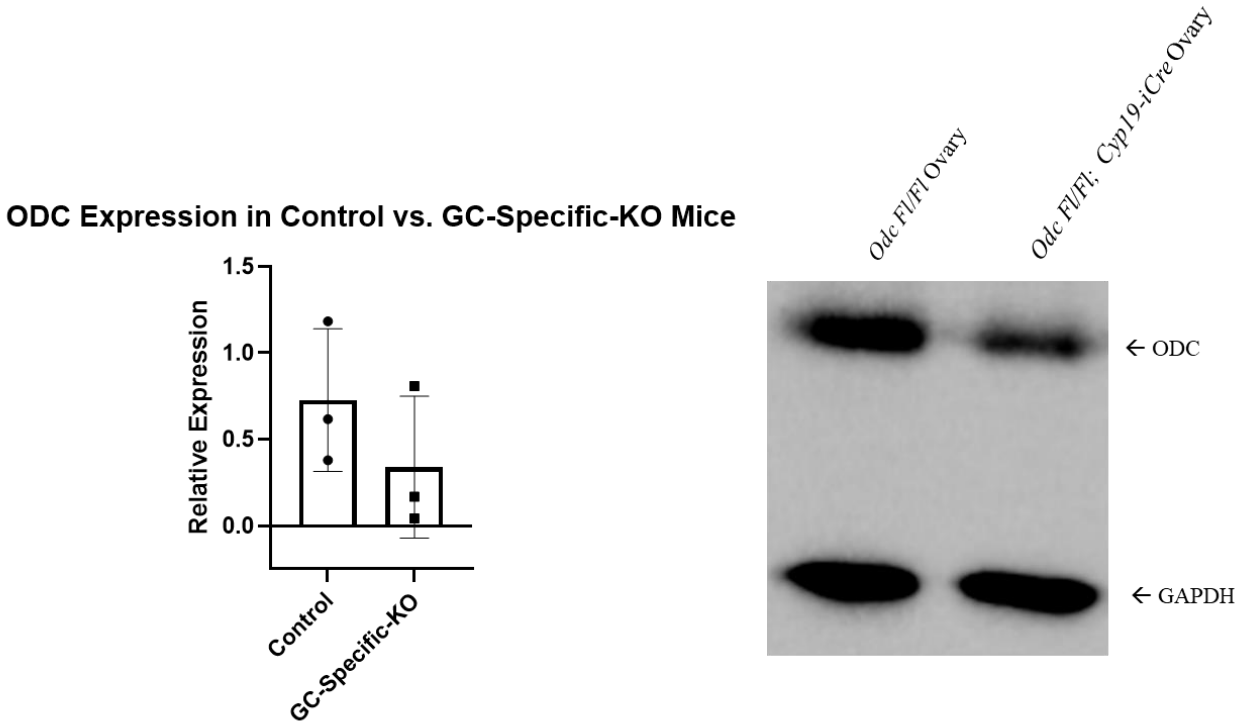

Figure 23. Representative western blot and quantitative analysis of ODC expression in granulosa cell-specific *Odc*-KO vs. control mice using 1000X ODC and 2000X GAPDH specific antibodies (N=3).
Western blot done using a monoclonal mouse ODC antibody and a monoclonal mouse GAPDH antibody as a housekeeping gene against stimulated ovaries taken from a granulosa cell-specific *Odc*-KO mouse and a control sister. Two trials were done using whole ovary tissue, while one was done using collected GC. A T test showed no significant difference in ODC expression in the KO mouse when compared to the control (P=0.3134).

3.2.4 Granulosa Cell-Specific *Odc*-KO Fluorescence-Activated Cell Sorting (FACS)

Due to the polyamine pathway being implicated in the cell cycle, fluorescence-activated cell sorting (FACS) using propidium iodide was done with collected granulosa cells from WT and GC-specific *Odc*-KO mice to determine what stage of the cell cycle they were in [36,41]. If putrescine production has been stopped then it is possible that this could affect the cell cycle of the GC and could be seen as an accumulation in one of the stages. From this analysis, it was found that the cell cycle proportions of GC from WT and *Odc*-KO-GC were nearly identical

(Fig. 24). Across both groups, approximately 80% of the cells were found to be in G1, 8% in S, and another 8% in G2/M phase. These results are different from other published data by approximately ±5%, with other studies finding 75% of GC to be in G1, 15% to be in S, and 10% to be in G2/M [34].

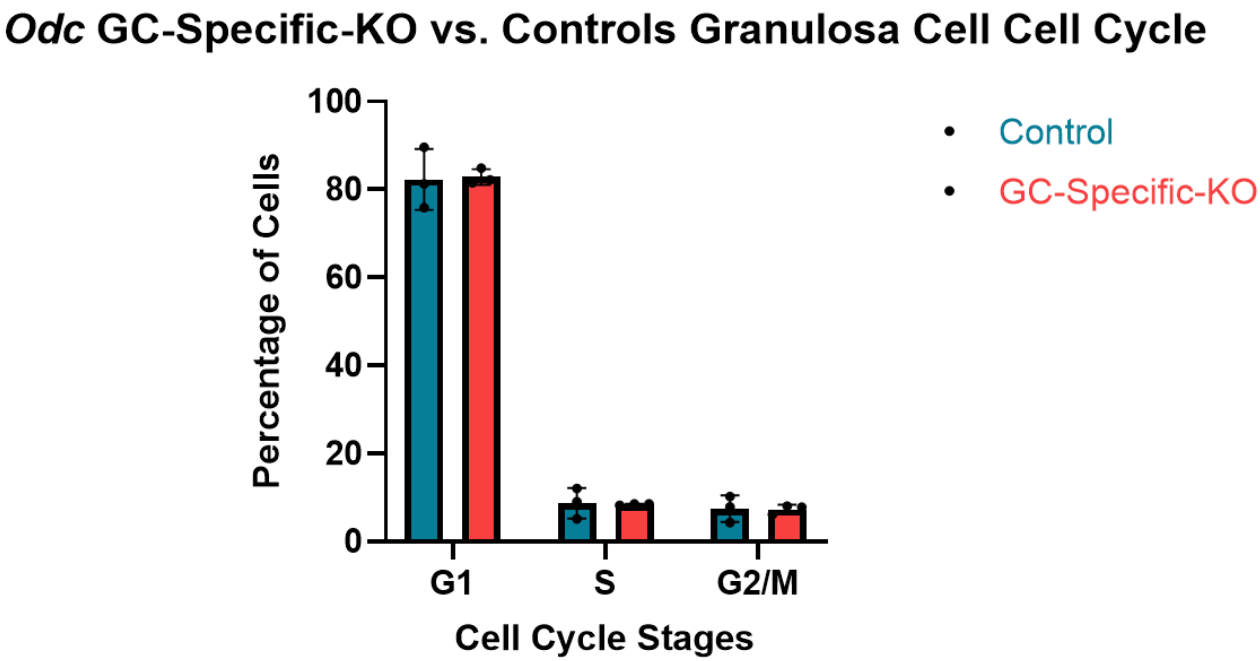

Figure 24. Cell cycle analysis of granulosa cells from wild-type and GC-specific *Odc*-KO mice using propidium iodide.
FACS cell cycle analysis using granulosa cells taken from PMSG stimulated females between 10-14wks-old. From PI staining no difference was found between the cell cycle of wild-type and GC-specific *Odc*-KO granulosa cells. Two-way ANOVA found no significant difference between the groups (P=0.9713).

3.2.5 Granulosa Cell-Specific *Odc*-KO Ovulation

Due to *Cyp19-iCre* expression beginning in the antral follicle stage, it was believed that knocking out *Odc* at this time in the GC could affect ovulation. In order to test this $Odc^{Fl/Fl}$; *Cyp19-iCre* and $Odc^{Fl/-}$; *Cyp19-iCre* females were superovulated. The mice were injected with

PMSG to induce follicle maturation and hCG to induce ovulation. 14 hours following the hCG injection the mice were sacrificed and the number of ovulated oocytes in the oviducts was counted. From this data, no significant difference was found in the number of oocytes ovulated by control mice versus $Odc^{Fl/Fl}$ GC-specific *Odc*-KOs (P=0.1373; Fig. 25a). Similarly, $Odc^{Fl/-}$ GC-specific *Odc*-KOs also showed no significant difference in the number of ovulated oocytes (P=5470; Fig. 25b).

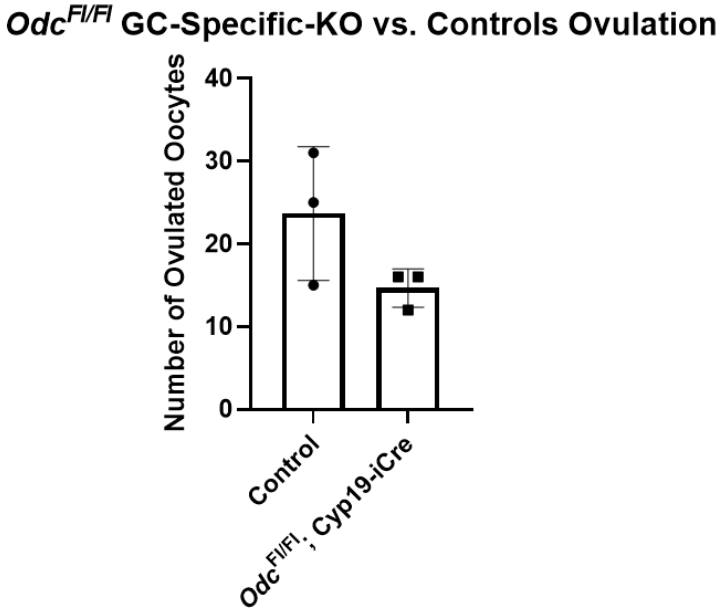

Figure 25a. Average number of ovulated oocytes from 6-8-week-old *Odc*$^{Fl/Fl}$*; Cyp19-iCre* GC-specific *Odc*-KO and control females.(N=3)

Average number of ovulated oocytes collected from the oviducts of three *Odc*$^{Fl/Fl}$ GC-specific *Odc*-KO females aged 6-8wks and three wild-type sisters ages 6-8wks. Conducting a T-test found no significant difference between the two groups (P=0.1373).

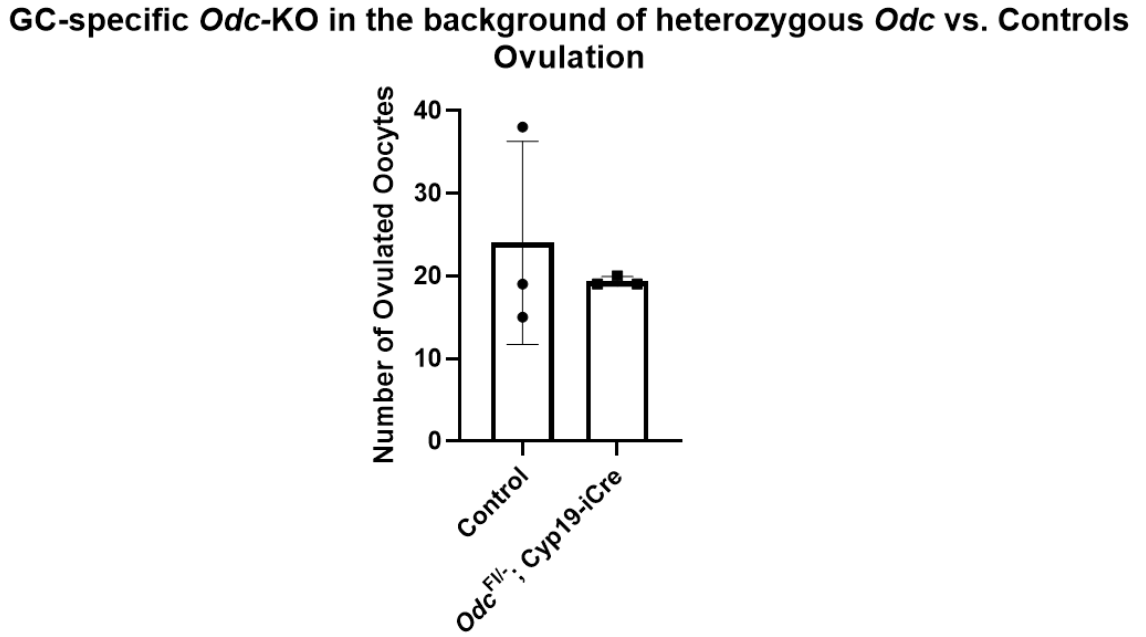

Figure 25b. Average number of ovulated oocytes from 6-8-week-old *Odc*$^{Fl/-}$*; Cyp19-iCre* GC-specific *Odc*-KO and control females.(N=3)

Average number of ovulated oocytes collected from the oviducts of three *Odc*$^{Fl/-}$ GC-specific *Odc*-KO females aged 4-6wks and three wild-type sisters ages 4-6wks. Conducting a T-test found no significant difference between the two groups (P=0.5470).

3.2.6 Granulosa Cell-Specific *Odc*-KO Fertility

To test the fertility of the GC-specific *Odc*-KO mice, females confirmed to $Odc^{Fl/Fl}$; *Cyp19-iCre* or $Odc^{Fl/-}$; *Cyp19-iCre* via PCR-genotyping were selected to go into breeding. At the same time, an $Odc^{Fl/Fl}$ sister that did not carry *Cyp19-iCre* was also put into breeding as a control. These mice were paired with males from the colony who did not carry *Cyp19-iCre*. The mice were kept in breeding for a prolonged period of time to see if the GC-specific *Odc*-KO had a premature reproductive phenotype.

3.2.6.1. $Odc^{Fl/Fl}$; *Cyp19-iCre* GC-Specific *Odc*-KO Long-Term Breeding Results

For the $Odc^{Fl/Fl}$ GC-specific *Odc*-KO mice, breeding lasted from eight weeks old to 43 weeks old. In this time the pairs were able to have between five to six litters. During breeding one of the GC-specific *Odc*-KO females had to be euthanized following the birth of her fifth litter due to mastitis. While in breeding there were no large gaps of time between litters to suggest that the mice were having any kind of complications. As seen in figure 26b, no significant difference was observed between the litters on average (P=0.5068). Additionally, no significant difference was seen in the birth weight of the pups (P=0.4177; Fig. 27)

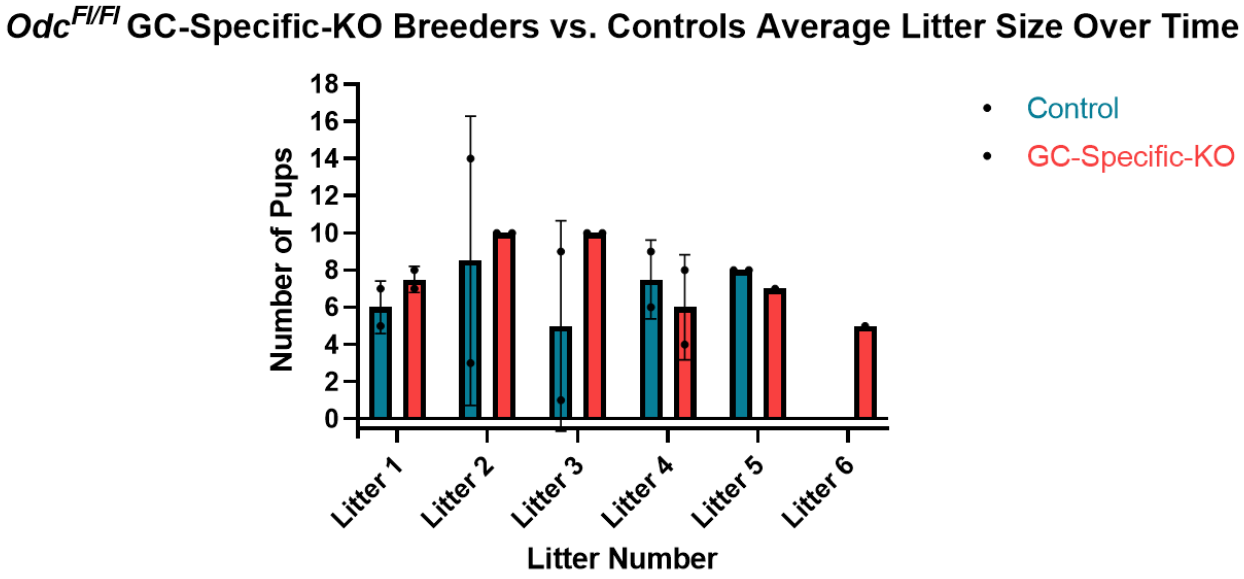

Figure 26a. Average litter size by litter number of control females versus GC-specific *Odc*-KO females in long-term breeding.

Average litter size of two GC-specific *Odc*-KO females with the genotype *Odc*$^{Fl/Fl}$; *Cyp19-iCre*, versus the average litter size of two wild-type sisters. Mice were in breeding from March 22nd, to Nov 24th, 2022.

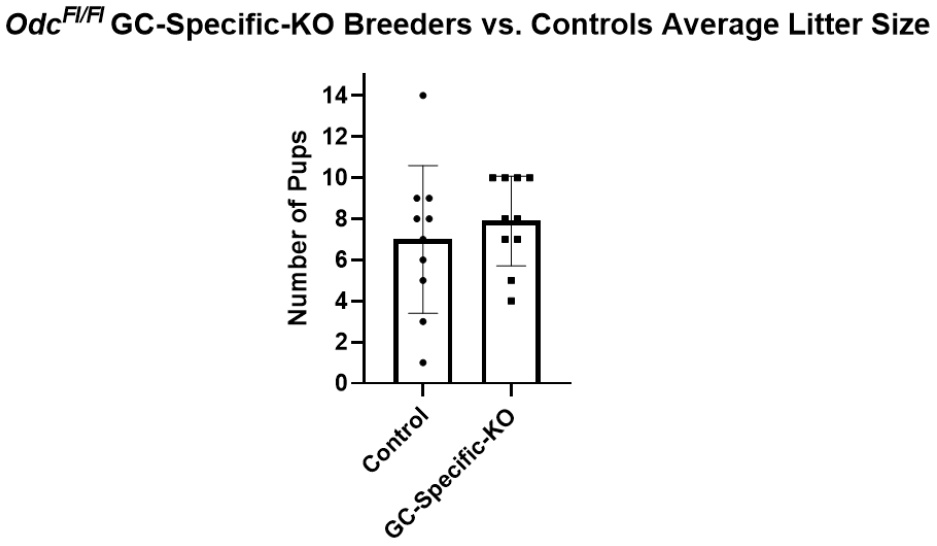

Figure 26b. Average litter size of control females versus GC-specific *Odc*-KO females in long-term breeding. (Control: N=10, KO: N=10)

Average litter size of two GC-specific *Odc*-KO females with the genotype *Odc*$^{Fl/Fl}$; *Cyp19-iCre*, versus the average litter size of two wild-type sisters. Mice were in breeding from March 22nd, to Nov 24th, 2022. In this time that the mice have been in mating no significant difference was observed between control and KO litters. A T-test found no significant difference between groups (P=0.5068).

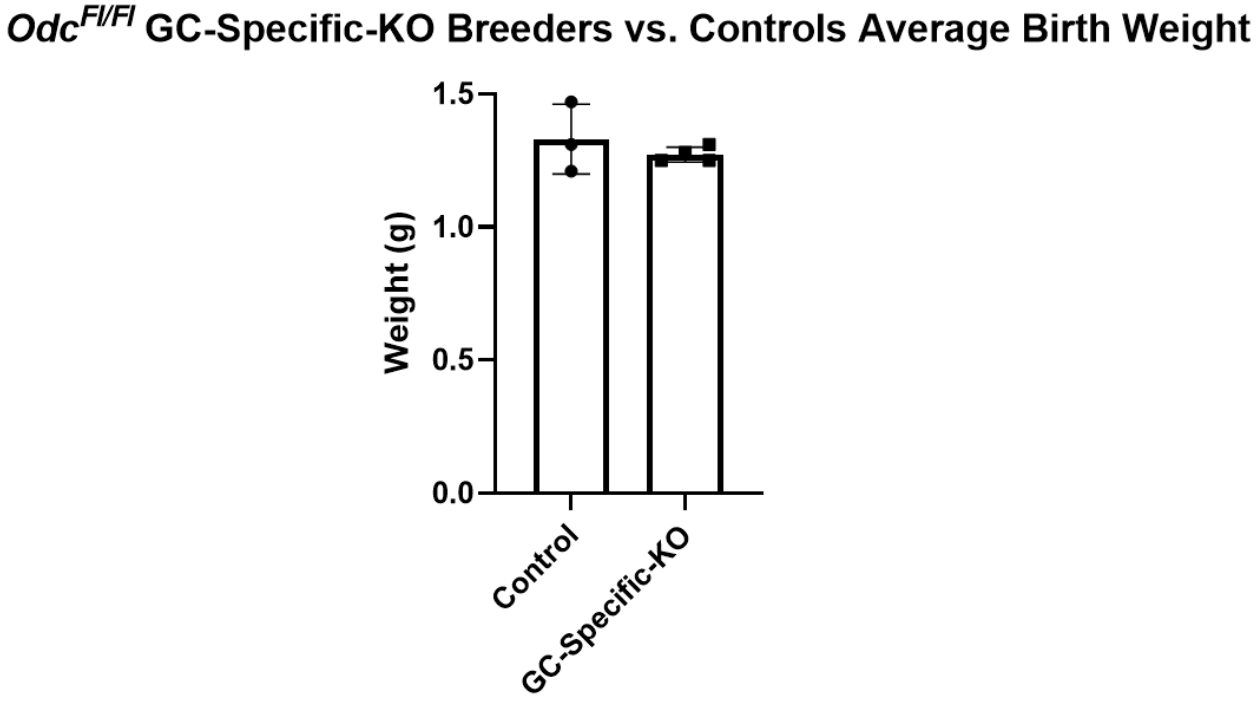

Figure 27. Average birth weight of control female litters versus GC-specific *Odc*-KO female litters in long-term breeding. (Control: N=3, KO: N=4)
Average birth weight of litters from two GC-specific *Odc*-KO females with the genotype $Odc^{Fl/Fl}$; *Cyp19-iCre*, versus the average birth weight of litters from two wild-type sisters. Mice were in breeding from March 22nd, to Nov 24th, 2022. In the time that the mice were in mating no significant difference was observed in the birth weight of pups born to either group (P=0.4177).

3.2.6.2. $Odc^{Fl/-}$; *Cyp19-iCre* GC-Specific *Odc*-KO Long-Term Breeding Results

To test the GC-specific *Odc*-KO in the background of heterozygous *Odc*, three GC-specific *Odc*-KO females were put into breeding when they were between eight and nine weeks old, against three $Odc^{Fl/Fl}$ control sisters. These mice were in breeding until they were between 28-30 weeks old. During this time, they were each able to have four to five litters with no large gaps of time between them. While in breeding one of the control females died due to complications during the birth of her second litter. Litter size showed no significant difference on average (P=0.5326; Fig. 28b)

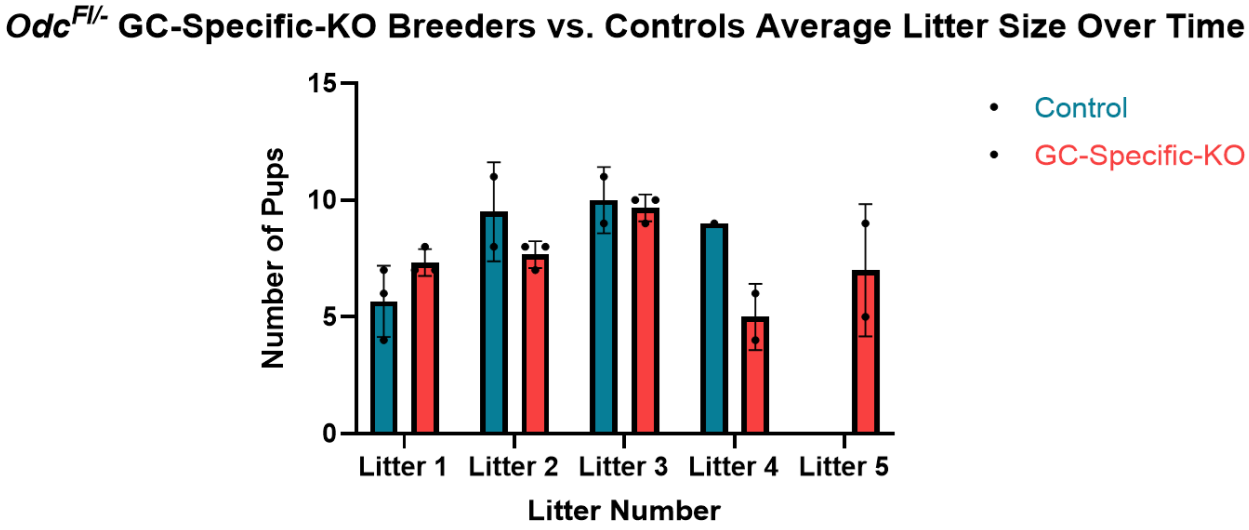

Figure 28a. Average litter size over time of control females versus *Odc Fl/-; Cyp19-iCre* GC-specific *Odc*-KO females in long-term breeding.
Average litter size of three females with the genotype $Odc^{Fl/-}$; *Cyp19-iCre*, versus the average litter size of three wild-type sisters. Mice were in breeding from March 22nd, to Nov 24th, 2022.

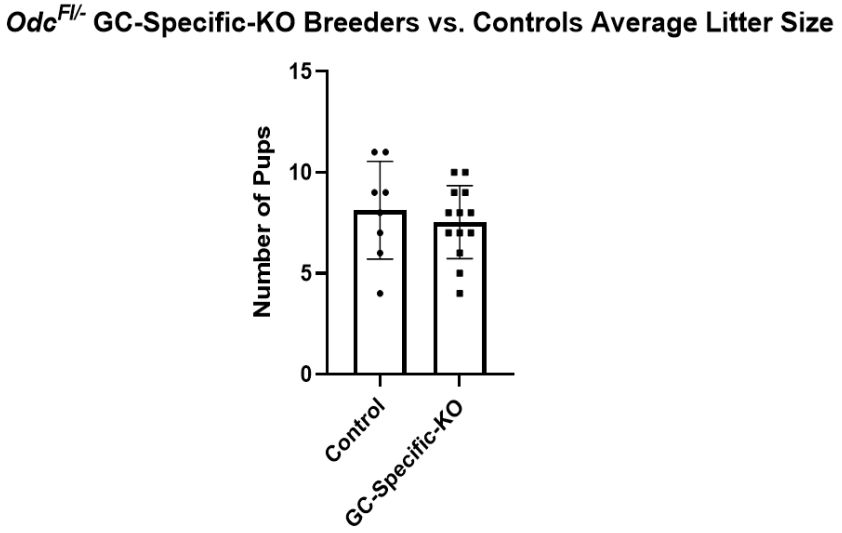

Figure 28b. Average litter size of control females versus *Odc Fl/-; Cyp19-iCre* GC-specific *Odc*-KO females in long-term breeding. (Control: N=8, KO: N=13)
Average litter size of three females with the genotype $Odc^{Fl/-}$; *Cyp19-iCre*, versus the average litter size of three wild-type sisters. Mice were in breeding from March 22nd, to Nov 24th, 2022. In the time that the mice were in mating no significant difference was observed between control and KO litters. A T-test found no significant difference between the groups (P=0.5326).

3.3. Oocyte, and GC-Specific Double *Odc*-KO Mice

3.3.1. Oocyte, and GC-Specific Double *Odc*-KO Genotyping

As no phenotype was seen in the fertility of mice who had *Odc* knocked out in the oocytes or GC alone, double *Odc*-KO mice, which had *Odc* knocked out in both the oocytes and GC were bred. PCR-genotyping was done using the same primers used to identify the GC and oocyte-specific *Odc*-KO mice. As seen in figure 29, these oocyte and GC-specific *Odc*-KO mice had *Odc* knocked out in the background of heterozygous *Odc* (*$Odc^{Fl/-}$; Cyp19-iCre; GDF9-iCre)*.

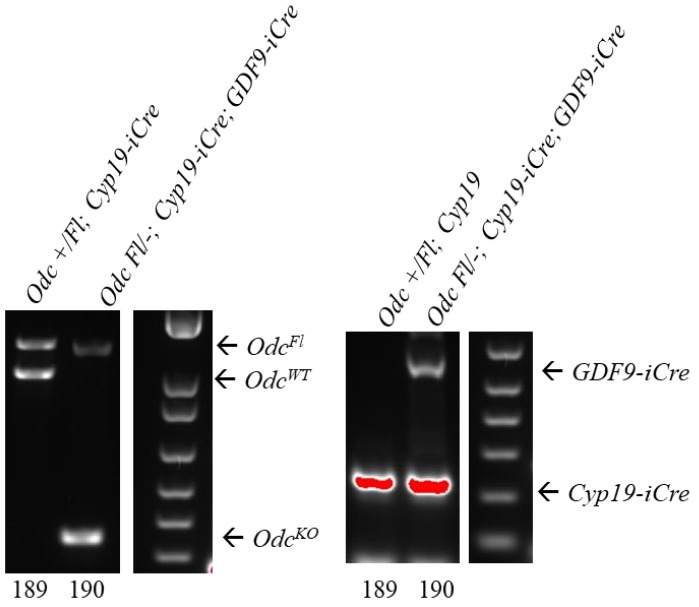

Figure 29. PCR of an oocyte, and GC-specific double *Odc*-knockout mouse and an *$Odc^{+/Fl}$; Cyp19-iCre* sister for comparison. The band indicating *Odc^{Fl}* can be found around 1122bp, the *Odc^{WT}* band around 1018bp, the *Odc* deletion around 300bp. The band for *Cyp19-iCre* can be found at 290bp and the *GDF9-iCre* band at 732bp.

3.3.2. Oocyte, and GC-Specific Double *Odc*-KO Breeding

In order to test the fertility of these oocyte and GC-specific *Odc*-KO mice, two were put into breeding with *$Odc^{Fl/Fl}$* males. Two *$Odc^{Fl/Fl}$* sisters were also put into breeding as controls. The mice were in breeding from eight weeks old to 34 weeks old. In this amount of time, they

were able to have between three to five litters with no significant gaps of time between litters. While in breeding one of the control females was euthanized due to complications in giving birth to her second litter. No significant difference was observed in the number of pups born between the KO and control breeders in litter size (P=0.1089).

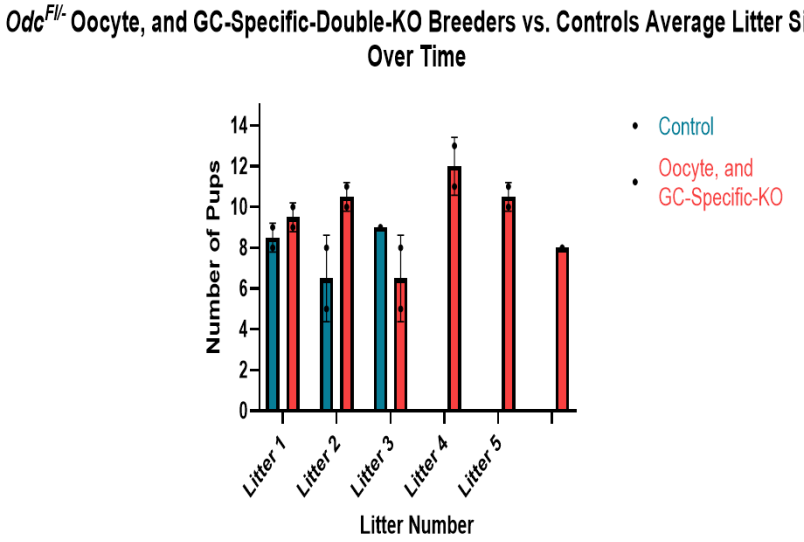

Figure 30a. Average litter size over time of control females versus oocyte and granulosa cell-specific double *Odc*-knockout females in long-term breeding.

Average litter size over time of two oocyte, and GC-specific double *Odc*-KO females with the genotype $Odc^{Fl/-}$; *Cyp19-iCre*; *GDF9-iCre*, versus the average litter size of two $Odc^{Fl/Fl}$ sisters. Mice were in breeding from May 24th, until Nov 24th, 2022.

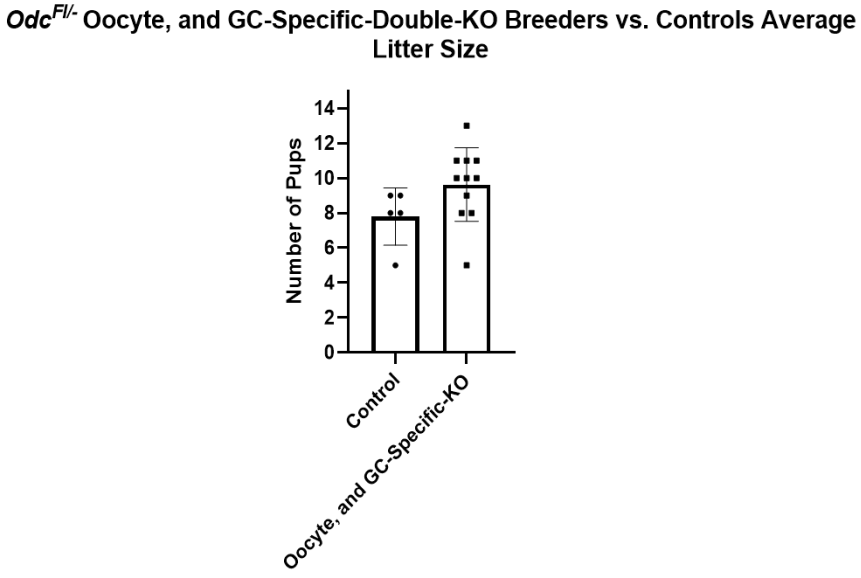

Figure 30b. Average litter size of control females versus oocyte and granulosa cell-specific double Odc-knockout females in long-term breeding. (Control: N=5, KO: N=11)

Average litter size of two oocyte, and GC-specific double *Odc*-KO females with the genotype $Odc^{Fl/-}$; *Cyp19-iCre*; *GDF9-iCre*, versus the average litter size of two $Odc^{Fl/Fl}$ sisters. Mice were in breeding from May 24th, until Nov 24th, 2022. In the time that the mice were in mating no significant difference was observed between control and KO litters (P=0.1089).

4. Discussion

Many *in vivo* studies of the effects of ODC and polyamines during reproduction have been conducted using the chemical inhibitor DFMO. Fozard *et al* applied DFMO in order to study polyamines during ovulation, as well as embryogenesis. While their work showed that inhibiting ODC during embryogenesis had a significant effect, inhibiting polyamine production during ovulation proved to be not as impactful [11]. Despite showing that DFMO did indeed block polyamine production, and by extension prevent the preovulatory rise in ovarian ODC activity, negative effects were only seen in the mean fetal and placental weight [12]. In 2005 Bastida *et al* once again employed DFMO in order to study the effects of polyamines on reproduction, choosing to focus on ovarian development and hormone regulation. In their studies, they found that when 24-day-old mice were injected with DFMO (500mg/kg), as well as having it supplemented in their drinking water, ovarian development and antral follicle development were negatively affected [4].

Throughout all of these *in vivo* studies, the effect of ODC and polyamines on the oocyte is neglected, with Bastida *et al* commenting that while ODC is expressed in oocytes across all stages of development, its relevance is still unknown. During the experiments done by Fozard and Bastida, DFMO was applied either through intraperitoneal injection, by supplementing drinking water, or both. While these methods have proven valuable in researching the role of polyamines during reproduction, it is impossible to know if the inhibitor has reached a critical concentration in the oocytes to block ODC activity there. Using *GDF9-iCre*, we are able to knock out *Odc* in oocytes with more precision than what could be achieved with chemical methods. Through these oocyte-specific *Odc*-KO mice, we have been able to show that *Odc* expression within the oocyte is not required for oogenesis or follicular development.

When examining total RNA extracted from collected GV/GVBD oocytes via RT-PCR, those that had been collected from the oocyte-specific *Odc*-KO mice produced only a truncated PCR product (Fig. 9). This truncated PCR product demonstrates that *GDF9-iCre* was able to loop out exons 2 and 3 successfully. The start codon of *Odc* resided in exon 3 [18]. With this start codon gone *Odc* should no longer be able to synthesize its protein product, the enzyme ODC. In order to validate that this was the case western blot was done. From western blot, we were able to show that oocytes collected from the oocyte-specific *Odc*-KO mice did indeed have a great reduction in ODC expression when compared to WT controls (Fig. 11). The quantitative analysis of the nitrocellulose membrane further validates this conclusion.

Despite this clear result that *GDF9-iCre* was able to loop out exons 2 and 3, stopping the translation of *Odc*, no impact on the fertility of the mice was observed. While breeding the oocyte-specific *Odc*-KO mice no difference was observed between WT-control breeders and oocyte-specific *Odc*-KO breeders in the number of pups born (Fig. 17b), or the birth weight of the pups (Fig. 18). This result did not change as the mice were reaching old age (Fig. 17a). The lack of phenotype could also be seen in the histology of the oocyte-specific *Odc*-KO mice, as follicle counting of eight-week-old and 42–44-week-old oocyte-specific *Odc*-KOs and WT-controls showed no significant difference in the number of follicles across all stages of development. Additionally, when old breeders (42-44 weeks of age) were superovulated no difference was observed in the number of oocytes ovulated between WT controls and oocyte-specific *Odc*-KOs.

One could suggest that a truncated ODC, resulting from internal translation initiation in the absence of the ATG codon on exon 3, might be produced and evades detection by the anti-ODC antibodies used. However, work with *Odc*-null mice by Pendeville *et al* also targeted the

same exons 2 and 3 yielding dramatic results, suggesting that this hypothetical truncated ODC product, if present, is not functional [32]. A more probable explanation for this result is the connection between oocytes and GCs through gap junctions. As stated previously gap junctions are intercellular pathways which allow the passage of molecules that are less than 1kDa in size between the GC and between the GC and the oocyte. The synthesis of GDF9 begins in the oocyte during the primordial stage of oocyte development. At this stage a layer of squamous pre-granulosa cells is present and gap junctions are already formed linking the oocyte to the GC [29,40]. Putrescine, the product of ODC, is 88.15Da. This size is well within the range for passage between gap junctions. Additionally, the other subsequent products of the polyamine pathway, spermidine and spermine, are within the size range for transport through the gap junctions. The polyamine pathway is also reversible with spermine being able to synthesize spermidine and spermidine being able to synthesize putrescine [23]. By utilizing these gap junctions, the oocyte could have *Odc,* and as a result, the polyamine pathway knocked out but not be at risk for polyamine depletion. Alternatively, polyamines in the oocytes may be not required for oocyte development, maturation, and normal fertility. While the gap junctions are large enough to transport small molecules such as the polyamines, they are not large enough to transport ODC itself. Unlike its product putrescine, ODC is much larger being around 55kDa [20]. Due to its size, it is far too large to pass through the gap junctions and into the oocyte.

While *GDF9-iCre* was successful in looping out exons 2 and 3 in the oocytes, *Cyp19-iCre* did not offer the same results. Unlike the *Odc*-KO oocytes which produced only a truncated PCR product during RT-PCR, granulosa cells collected from GC-specific *Odc*-KO mice produced both an intact WT band and a truncated band that had exons 2 and 3 removed (Fig. 21). These results suggested that *Cyp19-iCre* was not able to delete *Odc* in all of the GC. In order to

better quantify this, we turned to RT-qPCR. The results of RT-qPCR not only validated the partial-GC-specific *Odc*-KO seen in RT-PCR but also showed variability in the degree of KO between each mouse (Fig.22a). Based on the results obtained from RT-qPCR *Cyp19-iCre* was only able to loop out exons 2 and 3 in approximately 35% of GC in $Odc^{Fl/Fl}$*; Cyp19-iCre* mice. However, this partial-GC-specific *Odc*-KO was still shown to be able to reduce the expression of ODC to some degree. Results from western blot using whole ovaries, as well as GC directly, showed expression of ODC was reduced when comparing WT-controls and GC-specific *Odc*-KOs, although once again with some level of variability between repeats (Fig. 23).

With the results seen from this partial-GC-specific *Odc*-KO, it is not surprising that it was found to have no observable effect on the fertility of the mice. Breeding data collected from two $Odc^{Fl/Fl}$*; Cyp19-iCre* mice (Fig. 26), and three $Odc^{Fl/-}$*; Cyp19-iCre* mice (Fig. 28), as well as ovulation data from both groups (Fig. 25), showed no significant difference between the GC-specific *Odc*-KO and WT-controls. However, due to this only being a partial-GC-specific *Odc*-KO we are unable to be certain on the effects of deleting *Odc* in the GC.

Just as in the oocyte, the gap junctions present a problem when trying to eliminate the polyamine pathway in the GC. Unlike GDF9 which is expressed early on in oocyte development, at the primordial follicle stage, Cyp19 is expressed later, in the antral follicle stage. By this point in time, the follicle has acquired serval layers of GC containing hundreds of thousands of cells [35]. If *Cyp19-iCre* is only able to knock out *Odc* in approximately 35% of the GC in $Odc^{Fl/Fl}$*; Cyp19-iCre* mice, there are still 65% of the GC that are able to synthesize polyamines and transfer them throughout the follicle. In order to study the effects of *Odc* on fertility the transport of polyamines through the gap junctions would need to be addressed. This would require the deletion of *Odc* in both the GC and the oocyte. However, the partial-GC-specific *Odc*-KO seen

in the *Cyp19-iCre* mice would render an oocyte and GC-specific double *Odc*-KO using this promotor ineffective, as polyamines would still be able to be transported throughout the follicle. A next step for these oocyte and GC-specific *Odc*-KO mice would be to collect both oocytes and GCs in order to perform RT-PCR, RT-qPCR, and western blot, to see how they compare to the KOs in oocytes or GC alone. An *in vitro* method of addressing the transport of polyamines through the gap junctions would be by incubating WT and oocyte-specific *Odc*-KO follicles in the presence of gap junction blockers, such as carbenoxolone (CBX) or 18α-glycyrrhetinic acid (AGA) [40]. These chemicals are non-specific blockers of gap junction communication. By culturing follicles from oocyte-specific *Odc*-KO mice alongside WT controls in the presence of these blockers we may be able to see a difference in oocyte or follicular development.

There is a possibility that the *Odc*-KO oocytes or granulosa cells were able to take up polyamines produced by the microbiome or supplied through the diet. However, previous work done by our lab found that feeding mice putrescine rich foods, such as green pepper, had no significant impact on tissue polyamine levels, suggesting that the putrescine supplied by diet was either poorly absorbed or poor bioavailability [39]. Additionally, when studying the embryonic lethality of *Odc*-null mice, Pendeville *et al* experimented with supplementing the mothers with putrescine in their drinking water during gestation. They found that putrescine supplementation did not significantly change the early embryonic lethality phenotype [32].

Due to ODC and polyamines being implicated in the cell cycle, it was hypothesized that knocking out *Odc* in the GC may have some effect on the cell cycle [41]. From our results of cell cycle analysis using PI staining, knocking out *Odc* in the GC using *Cyp19-iCre* had no effect on the cell cycle of the GC. However, these results cannot be used to rule out a link between *Odc* and GC proliferation. Not only did *Cyp19-iCre* result in only a partial-GC-specific *Odc*-KO, as

mentioned previously, in cell lines polyamine depletion was shown to not occur immediately. Instead, it was found that it took several cycles for polyamine concentration to reduce to a level where the cell cycle was affected [3]. In addition to polyamines moving through the gap junctions, *Cyp19-iCre* is not expressed until the antral follicle stage. At this point, it may be too late in development to see an observable difference in the cell cycle, as depletion has begun too late. In order to test this hypothesis an earlier and more reliable method of knocking out *Odc* in the GC, alongside the oocyte would be required. Alternatives to *Cyp19-iCre,* such as *Amhr2-iCre* would need to be investigated. *Amhr2* gene expression occurs much earlier in GC development than the *Cyp19* gene, hence an *Amhr2* promoter-driven iCre is expected to delete the *Odc* gene in GCs earlier during follicle development.

5. Conclusion

With these oocyte-specific *Odc*-KO mice, we have been able to study *in vivo* the effects of ODC and polyamines specifically on the oocyte. From the oocyte-specific *Odc*-KO mice, it has been found that *Odc* expression from within the oocyte is not required for oogenesis or follicular development. When compared to WT controls no difference was found in the fertility of the oocyte-specific *Odc*-KO mice, including into old age. Additionally, knocking out *Odc* in the oocytes was found to have no effect on the follicle numbers. Despite this lack of phenotype, *GDF9-iCre* has shown to be a reliable method of knocking out genes in the oocyte, as RT-PCR and western blot showed the successful deletion of *Odc* and the subsequent reduction of its protein. On the other hand, *Cyp19-iCre* has shown to be unreliable, as RT-qPCR found that *Cyp19-iCre* was only capable of a partial-GC-specific *Odc*-KO. Additionally, this incomplete-GC-specific *Odc*-KO was found to have variability in its effectiveness between each mouse. While *Cyp19-iCre* was found to be more effective in the background of heterozygous *Odc*, there was still variability between repeats. Similar to the oocyte-specific *Odc*-KO, the GC-specific *Odc*-KO was found to have no impact on the fertility of the mice. This was seen in the litter sizes, and birth weights of the pups, as well as the cell cycle of the GC. Oocyte and GC-specific *Odc*-KO mice were also found to have no difference in litter size when compared to WT controls. This lack of phenotype seen in the oocyte-specific *Odc*-KOs, the GC-specific *Odc*-KOs, and the oocyte and GC-specific *Odc*-KOs could be due to the products of the polyamine pathway, putrescine, spermidine, and spermine, being able to move freely through the gap junctions of the follicle. Further considerations on a reliable method of knocking out *Odc* in the GC are required to truly see the impact of knocking out *Odc* in the follicle.

6. Bibliography

1. Ajayi, A., & Akhigbe, R. (2020). Staging of the estrous cycle and induction of estrus in experimental rodents: an update. *Fertil Res and Pract, 6*(5), 1-15.
2. Albertini, D. F. (2015). The Mammalian Oocyte. In T. M. Plant, & A. J. Zeleznik, *Knobils and Neills Physiology of Reproduction* (4 ed., pp. 59-97). Amsterdam: Elsevier .
3. Alm, K., & Oredsson, S. (2009). Cells and polyamines do it Cyclically. *Biochem. Soc. Essays, 46*, 63-76.
4. Bastida, C. M., Cremades, A., Castells, M. T., Lopez-Contreras, A. J., Lopez-Garcıa, C., Tejada, F., & Penafiel, R. (2005). Influence of Ovarian Ornithine Decarboxylase in Folliculogenesis and Luteinization. *Endocrinology, 146*(2), 666-674.
5. Bromfield, J. J., & Piersanti, R. L. (2019). Mammalian Oogenesis: The Fragile Foundation of the Next Generation. In P. C. Leung, & E. Y. Adashi, *The Ovary* (3 ed., pp. 157-164). London, UK: Elsevier Inc.
6. Centers for Disease Control and Prevention. (2019). *2019 Assisted Reproductive Technology (ART) Fertility Clinic and National Summary Report.* Atlanta: U.S. Department of Health & Human Services.
7. Cohen, P. E., & Holloway, J. (2015). Mammalian Meiosis. In T. Plant, & A. Zeleznik, *Knobil and Neill's Physiology of Reproduction* (4 ed., pp. 5-57). Amsterdam: Elsevier.
8. Dong, J., Albertini, D. F., Nishimori, K., Kumar, R. T., Lu, N., & Matzuk, M. M. (1996). Growth differentiation factor-9 is required during early ovarian folliculogenesis. *Letters to Nature, 383*, 531-535.
9. El-Hayek, S., & Clarke, H. J. (2015). Follicle-Stimulating Hormone Increases Gap Junctional Communication Between Somatic and Germ-Line Follicular Compartments During Murine Oogenesis. *Biol. Reprod., 93*(2), 1-10.
10. Fan, H.-Y., Shimada, M., Liu, Z., Cahill, N., Noma, N., Wu, Y., . . . Richards, J. S. (2008). Selective expression of KrasG12D in granulosa cells of the mouse ovary causes defects in follicle development and ovulation. *Development, 135*(12), 2127-2137.
11. Fozard, J. R., Part, M.-L., Prakash, N. J., Grove, J., Schechter, P. J., Sjoerdsma, A., & Koch-Weser, J. (1980). L-Ornithine Decarboxylase: An Essential Role in Early Mammalian Embryogenesis. *Science, 208*(4443), 505-508.
12. Fozard, J. R., Prakash, N. J., & Grove, J. (1980). Ovarian Function in the Rat Following Irreversible Inhibition of L-Ornithine Decarboxylase. *Life Sci, 27*, 2277-2283.
13. Glick, I., Kadish, E., & Rottenstreich, M. (2021). Management of Pregnancy in Women of Advanced Maternal Age: Improving Outcomes for Mother and Baby. *Int J Womens Health., 13*, 751-759.

14. Hardbower, D. M., Asim, M., Luis, P. B., Singh, K., Barry, D. P., Yang, C., . . . Wilson, K. T. (2017). Ornithine decarboxylase regulates M1 macrophage activation and mucosal inflammation via histone modifications. *PNAS, 114*(5), E751-E760.

15. Igarashi, K., & Kashiwagi, K. (2010). Modulation of cellular function by polyamines. *Int. J. Biochem. Cell Biol., 42*, 39-51.

16. Jones, R. E., & Lopez, K. H. (2006). The Female Reproductive System. In R. E. Jones, & K. H. Lopez, *Human Reproductive Biology* (3 ed., pp. 31-72). Burlington, MA, USA: Elsevier.

17. Jones, R. E., & Lopez, K. H. (2006). The Menstrual Cycle. In R. E. Jones, & K. H. Lopez, *Human Reproductive Biology* (3 ed., pp. 73-96). Burlington, MA, USA: Elsevier.

18. Katz, A., & Kahana, C. (1988). Isolation and Characterization of the Mouse Ornithine Decarboxylase Gene. *J. Biol. Chem. , 263*(16), 7604-7609.

19. Kidder, G. M., & Mhawi, A. (2002). Gap junctions and ovarian folliculogenesis. *Reproduction, 123*, 613-620.

20. Kitani, T., & Fujisawa, H. (1983). Purification and Properties of Ornithine Decarboxylase from Rat Liver. *JBC, 258*(1), 235-239.

21. Kobayashi, Y., Kupelian, J., & Maudsley, D. V. (1971). Ornithine Decarboxylase Stimulation in Rat Ovary by Luteinizing Hormone. *Science, 172*(3981), 379-380.

22. Lan, Z.-J., Xu, X., & Cooney, A. J. (2004). Differential Oocyte-Specific Expression of Cre Recombinase Activity in GDF-9-iCre, Zp3cre, and Msx2Cre Transgenic Mice. *Biol. Reprod., 71*, 1469-1474.

23. Li, J., Meng, Y., Wu, X., & Sun, Y. (2020). Polyamines and related signaling pathways in cancer. *Cancer Cel Int., 20*(539), 1-16.

24. Lobo, R. A. (2004). Menopause and Aging. In J. F. Strauss, & R. L. Barbieri, *Yen and Jaffe's Reproductive Endocrinology: Physiology, Pathology, and Clinical Managment* (5 ed., pp. 421-462). Philadelphia , PA, USA: Elsevier Saunders .

25. LoGiudice, N., Le, L., Abuan, I., Leizorek, Y., & Roberts, S. C. (2018). Alpha-Difluoromethylornithine, an Irreversible Inhibitor of Polyamine Biosynthesis, as a Therapeutic Strategy against Hyperproliferative and Infectious Diseases. *Med Sci (Basel)., 6*(12), 1-17.

26. Londero, A. P., Rossetti, E., Pittini, C., Cagnacci, A., & Driul, L. (2019). Maternal age and the risk of adverse pregnancy outcomes: a retrospective cohort study. *BMC Pregnancy Childbirth, 19*(261), 1-10.

27. Mehlmann, L. M., Saeki, Y., Tanaka, S., Brennan, T. J., Evsikov, A. V., Pendola, F. L., . . . Jaffe, L. A. (2004). The Gs-linked receptor GPR3 maintains meiotic arrest in mammalian oocytes. *Science, 10*(306), 1947-1950.

28. Nishimura, K., Shiina, R., Kashiwagi, K., & Igarashi, K. (2006). Decrease in Polyamines with Aging and Their Ingestion from Food and Drink. *J. Biochem., 139*, 81-90.

29. Pedersen, T., & Peters, H. (1968). Proposal for a Classification of Oocytes and Follicles in the Mouse Ovary. *J. Reprod. Fert., 17*, 555-557.

30. Pegg, A. E. (2006). Regulation of Ornithine Decarboxylase. *JBC, 281*(21), 14529-14532.

31. Pegg, A. E. (2016). Functions of Polyamines in Mammals. *JBC, 291*(29), 14904-14912.

32. Pendeville, H., Carpino, N., Marine, J.-C., Takahashi, Y., Muller, M., Martial, J. A., & Cleveland, J. L. (2001). The Ornithine Decarboxylase Gene Is Essential for Cell Survival during Early Murine Development. *Mol. Cell. Biol., 21*(19), 6549–6558.

33. Provencher, C., Milan, A., Hallman, S., & D'Aoust, C. (2018). *Fertility: Overview, 2012 to 2016.* Ottawa: Statistics Canada.

34. Quirk, S. M., Cowan, R. C., & Harman, R. M. (2006). The susceptibility of granulosa cells to apoptosis is influenced by oestradiol and the cell cycle. *J. Endocrinol., 189*, 441-453.

35. Rajkovic, A., Pangas, S. A., & Matzuk, M. M. (2006). Follicular Development: Mouse, Sheep, and Human Models. In E. Knobil, & J. D. Neill, *Knobil and Neill's Physiology of Reproduction* (3 ed., pp. 383-423). Amsterdam; Boston: Elsevier.

36. Ray, R. M., Zimmerman, B. J., McCormack, S. A., Patel, T. B., & Johnson, L. R. (1999). Polyamine depletion arrests cell cycle and induces inhibitors p21Waf1/Cip1, p27Kip1, and p53 in IEC-6 cells. *Am J Physiol., 276*(3), C684-C691.

37. Tao, Y., & Liu, X. (2013). Deficiency of ovarian ornithine decarboxylase contributes to aging-related egg aneuploidy in mice. *Aging Cell, 12*, 42-49.

38. Tao, Y., Liu, D., Mo, G., Wang, H., & Liu, J. (2015). Peri-ovulatory putrescine supplementation reduces embryo resorption in older mice. *Hum. Reprod., 30*(8), 1867-1875.

39. Tao, Y., Tartia, A., Lawson, M., Zelinski, M. B., Wu, W., Liu, J.-Y., . . . Liu, X. (2019). Can peri-ovulatory putrescine supplementation improve egg quality in older infertile women? *J Assist Reprod Genet., 36*(3), 395-402.

40. Teng, Z., Wang, C., Wang, Y., Huang, K., Xiang, X., Niu, W., . . . Zhang, H. (2016). Gap junctions are essential for murine primordial follicle assembly immediately before birth. *Reproduction, 151*(2), 105-115.

41. Veldhuis, J. A., & Hammond, J. M. (1979). Role of Ornithine Decarboxylase in Granulosa-Cell Replication and Steroidogenesis in Vitro. *BBRC, 91*(3), 770-777.

42. Wallace, H. M., Fraser, A. V., & Hughes, A. (2003). A perspective of polyamine metabolism. *Biochem. J., 376*, 1-14.

43. Zhang, M., Su, Y.-Q., Sugiura, K., Xia, G., & Eppig, J. J. (2010). Granulosa cell ligand NPPC and its receptor NPR2 maintain meiotic arrest in mouse oocytes. *Science, 15*(330), 366-369.

44. Zhou, Y., Ma, C., Karmouch, J., Arabi Katabi, H., & Liu, J. X. (2009). Antiapoptotic Role for Ornithine Decarboxylase during Oocyte Maturation. *Mol. Cell. Biol, 29*(7), 1786-1795.